Received: 13 April 2018 | Accepted: 15 June 2018

DOI: 10.1002/pcr2.10015

WILEY Polymer Crystallization

REVIEW

Crystal structures and polymorphism of polymers: Influence of defects and disorder

Claudio De Rosa | Finizia Auriemma | Anna Malafronte | Miriam Scoti

Dipartimento di Scienze Chimiche, Università di Napoli "Federico II" Complesso Monte S. Angelo, Via Cintia, I-80126, Naples, Italy

Correspondence
Claudio De Rosa, Dipartimento di Scienze Chimiche, Università di Napoli "Federico II," Complesso Monte S.Angelo, Via Cintia, I-80126 Naples, Napoli, Italy.
Email: claudio.derosa@unina.it

Abstract

The crystal structures and the polymorphism of polymers are described on the basis of the main principles that define the conformation of polymer chains in the crystalline state and the modes of packing of macromolecules. We show that the presence of defects and disorder in the crystals influences the polymorphic behavior. The cases of polymorphism of isotactic poly(butene) (iPB) and syndiotactic poly(styrene) (sPS) are ilustrated as examples. In the case of iPB, the effect of the presence of defects of stereoregularity and of comonomeric units on the crystallization of form I and form II is described as an example of alteration of the crystallization behavior because of the modification of both thermodynamic stability and crystallization kinetics from the melt of the polymorphic forms. The case of sPS is taken as an example of a very complex polymorphic behavior arising from the presence and development of structural disorder.

KEYWORDS

basic principles that define chain conformation and packing, crystal structures of polymers, influence of defects and disorder, isotactic poly(butene), polymorphism, symmetry breaking, syndiotactic poly(styrene)

1 | INTRODUCTION

Polymorphism is the ability of a polymer, in analogy with low molecular mass substances, to crystallize in different modifications, characterized by different crystal structures (polymorphic forms).[1–6] Almost all crystalline polymers show polymorphic behavior. The widespread observation of polymorphism in polymers precludes a discussion of each specific case,[7,8] but the phenomenon can be rationalized setting forth basic concepts and main principles that govern the crystallization of polymers, that is the formation of ordered conformational sequences of monomeric units and their packing in a crystalline lattice.[1]

In general, polymorphism in polymers can be divided in two broad categories. In the first category, different crystal forms of the same polymer arises from the fact that the chain molecules can assume different stable conformations in the crystalline state (*conformational polymorphism*) resulting in polymorphic forms characterized by different chain conformations packed in different unit cells.[1] In the second category, different crystal forms are characterized by chains with identical conformation packed in different unit cells and/or space group symmetries (*packing polymorphism*).[1]

The crystallization process can be easily described in terms of thermodynamic and kinetics aspects[7] and what drives the polymer toward the formation of a polymorph is often related to details, which are not easily rationalizable. Key roles are played by the molecular structure, the presence of molecular defects, the condition of crystallization, the presence of external bias, and so forth.

Different crystal structures can develop during crystallization from the melt by variation of temperature, pressure or presence of seeds acting as selective nucleating agent, and by application of deformation in tension or shear, or from polymer-diluent mixtures depending on the nature of the diluent and its concentration. When a polymer crystallizes in different polymorphic forms, it is also very common occurrence of phase transformations between the different polymorphs induced by variation of temperature[1,7] or by deformation upon application of tensile stress (stress-induced phase transition).[1,2,9] A common observation is that a phase transition occurs through steps of increasing thermodynamic stability (Ostwald's rule).[10–14] Different polymorphic modifications may also crystallize together without phase transformations of one into the other. Specially, they may nucleate independently and grow simultaneously.[15]

It is also common the nucleation of one polymorphic form on the crystals of a polymorphic form already formed.[16,17]

In this review we analyze the thermodynamic basis for conformational and packing polymorphisms neglecting the kinetics aspects. In particular, we describe several parameters and phenomena that influence the mode of packing of macromolecules and their role on driving crystallization of a particular polymorph, as the presence of defect and disorder in the crystal, the constraints imposed by chirality, the symmetry breaking and frustration, and the chiral crystallization.[1,2] The transformations between polymorphs induced by temperature and mechanical stresses are also described. The transformation can occur either by direct conversion of one form to the other or by melting of one form and the subsequent recrystallization of the other from the melt.

The determination of the free energy of melting for each of the forms, as a function of the intensive variable involved, is necessary to decide their relative stability, and the thermodynamic basis for the transformation.[7] However, it does not necessarily follow that the interconversion will follow the prescribed equilibrium path. The crystalline modification that is actually observed is a result of crystallization conditions and will be governed to a large extent by kinetic factors.[7] A schematic diagram of the free energy (at constant pressure) as a function of temperature of two polymorphic forms and of the liquid state of a polymer, shown in Figure 1, illustrates two possible modes of transformation of one form into the second form in a monotropic (Figure 1A) or enantiotropic (Figure 1B) polymorphism.[7] The temperature is taken as the sole intensive variable. In the case of monotropic polymorphism of Figure 1A, the polymorphic form I has the lowest free energy at all temperatures below its melting temperature, and, therefore, is the thermodynamically more stable crystal structure at all temperature. Form II is a metastable polymorphic form that melts at temperature T_{mII} lower than the melting temperature of form I (T_{mI}). This system does not undergo a crystal-crystal transformation between forms I and II with temperature. In the case of enantiotropic polymorphism of Figure 1B, each of the three phases is stable in a certain temperature range and form I is still the most stable polymorph at low temperatures, even though form II has now the higher melting temperature (T_{mII}). With increasing temperature the free energy curves of form II and form I intersect, so that the crystal-crystal transformation of form I into form II occurs at the intersection temperature ($T_{I\text{-}II}$). At this temperature, form II becomes the most stable polymorphic form up to its melting temperature (T_{mII}).

A condition for concomitant crystallization of two polymorphs in a monotropic system is that the crystallization must occur at low temperatures, lower than the melting temperature of form II (T_{mII} of Figure 1A), and a slow kinetics of crystallization of the stable polymorphic form (form I). This condition generally occurs in polymers because of the typical high undercooling. For enantiotropic system of Figure 1B, concomitant crystallization of forms I and II can be obtained at crystallization temperatures lower than the melting temperature of form I (T_{mI}).

Examples of metastable polymorphic forms of polymers, which can be obtained for instance by rapid cooling from the melt or by deformation of the stable polymorphic form, have been extensively described in the literature.[1,2,5,6,18] Most of these metastable forms have been described as solid mesophases and are characterized by different types of structural disorder that do not prevent crystallization.[1,2,5,6,18]

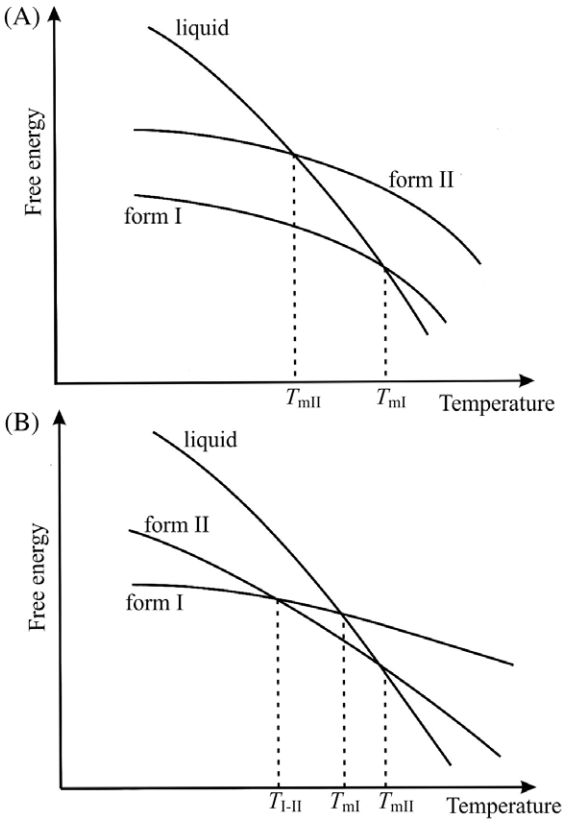

FIGURE 1 Schematic diagram of the free energy (at constant pressure) as a function of temperature of two polymorphic forms (forms I and II) and of the liquid state of the same polymer showing a monotropic (A) and enantiotropic (B) polymorphism[7]

For systems involving other intensive variables, such as pressure, stress, composition of a mixture, the free energy surfaces of the individual phases are treated in a similar manner. For example, the addition of a diluent to the liquid-phase results in a decrease of its free energy at all temperatures and a concomitant alteration of the stability conditions for each of the crystalline forms.[7] The case of the effect of pressure is well represented by the polymorphism of polyethylene that crystallizes in the stable orthorhombic form and in the metastable hexagonal form.[1,2,7] The schematic diagrams of the free energy at atmosphere pressure and high pressure, as a function of temperature of the two polymorphic forms of polyethylene are shown in Figure 2.[7,19] At atmosphere pressure, the orthorhombic form is the most stable form at all temperatures, up to its melting temperature T_m^{or} (Figure 2A), whereas the hexagonal form melting at temperature T_m^h lower than T_m^{or} has higher free energy at all temperatures. At high pressure, a crossover of the curves of the free energies of orthorhombic and hexagonal forms occurs at the temperature T_{or}^h, where the crystal-crystal transformation of the orthorhombic form into the hexagonal form occurs (Figure 2B). At this temperature the hexagonal form becomes the most stable polymorphic form up to its melting temperature T_m^h, which is higher than the transition temperature T_{or}^h and higher than the melting temperature of the orthorhombic form T_m^{or} (Figure 2B).[19]

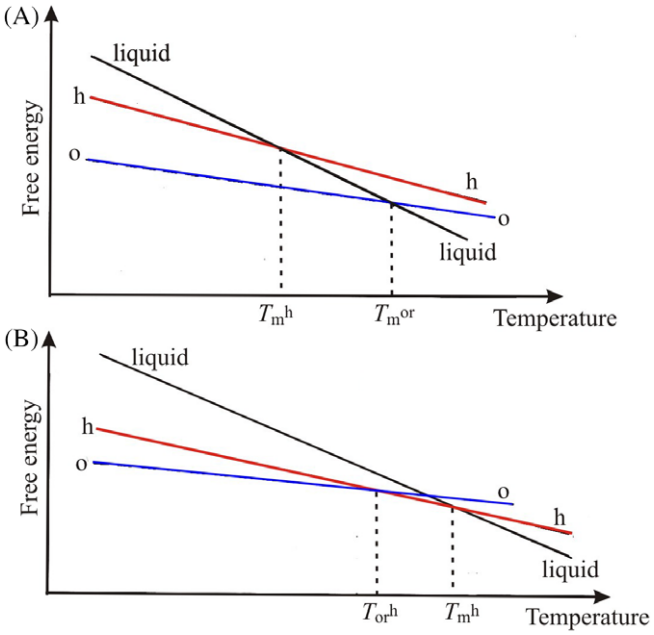

FIGURE 2 Schematic diagrams of the free energy at atmosphere pressure (A) and high pressure (B) as a function of temperature of the two polymorphic forms of polyethylene (o = orthorhombic form, h = hexagonal form)[19]

As mentioned above, besides intensive external parameters that define the condition of crystallization, molecular parameters, the crystal density and entropy of packing, and the presence of defects and disorder in the crystals, may define the diagrams of Figure 1, and alter the crystallization pathways. In the next sections, these parameters are discussed and, in particular, examples of the alteration of the polymorphic behavior of Figure 1 because of the presence of molecular defects (defects of stereoregularity and regioregularity in poly[1-olefins]) and of polymorphism arising from crystallization of disordered structures are provided. The cases of isotactic poly(butene) and syndiotactic poly(styrene) are discussed as examples.

The capability of polymers to crystallize (crystallizability) requires generally a regularity in the constitution of the macromolecules, in the configuration of the stereoisomeric centers (if present) and in the conformation of the chains.[1,3]

Small amounts of defects in the regular constitution and configuration may be in general tolerated and may not prevent crystallization. However, the presence of constitutional and/or configurational defects may influence the crystallization and, besides the decrease of crystallinity, in many cases may drive crystallization toward a polymorphic form by stabilizing that form and destabilizing other polymorphic forms.[1] The controlled incorporation of defects through methods of controlled polymerization has been exploited to tailor the physical and mechanical properties of polymers, as explained in the case isotactic[20–23] and syndiotactic polypropylene,[24–26] and isotactic polybutene (iPB).[27–30]

2 | ISOTACTIC POLYBUTENE

Isotactic poly(butene) (iPB) shows a complex polymorphic behavior of the type of Figure 1A. iPB crystallizes in three different polymorphic forms, defined forms I, II, and III, which are characterized by chains in different conformations and different crystal packing.[31–44] In the stable form I the chains assume the most stable 3/1 helical conformation and are packed in a trigonal unit cell with axes $a = b = 17.7$ Å and $c = 6.5$ Å, according with the space group $R3c$ or $R\bar{3}c$.[31,32] Form II is characterized by chains in 11/3 helical conformation packed in a tetragonal unit cell with axes $a = b = 15.42$ Å, $c = 21.05$ Å and space group symmetry $P\bar{4}$.[33–37] In the form III the chains are in the 4/1 helical conformation and are packed in an orthorhombic unit cell with axes $a = 12.38$ Å, $b = 8.88$ Å, $c = 7.56$ Å, and space group $P2_12_12_1$.[38–40] This is a typical example of conformational polymorphism that arises because of the possibility of the iPB macromolecules to assume in the crystalline state three different conformations of low energy resulting from small variations of the values of the nearly trans and nearly gauche dihedral angles along the main chain.[1] The 3/1, 11/3, and 4/1 helical conformations of the chains of iPB in the different polymorphic forms are shown in Figure 3.

The three conformations and the relative stabilities of the three different polymorphic forms have been interpreted by calculation of conformational energy.[35–37,45] In fact, two minima of the conformational energy have been found in the region of the helical conformation[35–37] for a chain of iPB under the constraints imposed by equivalence principle.[1–3] This principle imposes that, if θ_1 and θ_2 are the torsion angles of two successive bonds CH_2-CH and CH-CH_2 in two successive poly(1-olefins) monomeric units, successive monomeric units take equivalent conformations in the crystalline state and hence successive bonds assume the same torsion angles θ_1 and θ_2. The conformation is, therefore, easily described as a regular succession of torsion angles $(\theta_1\theta_2)_n$. For the chain of iPB, the absolute energy minimum has been observed for the 3/1 helix, found in the form I of iPB,[31] corresponding to a succession of torsion angles Trans (180°) and Gauche (60°), that is $(\theta_1\theta_2)_n = (TG)_n$. The 11/3 and 4/1 helices found in the forms II and III of iPB, respectively,[33–36,38] correspond

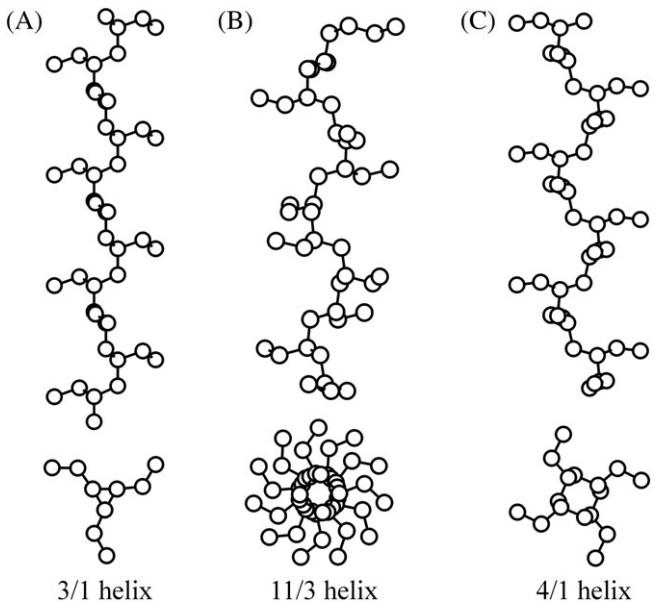

FIGURE 3 Chains of iPB in 3/1 (A), 11/3 (B), and 4/1 (C) helical conformations that crystallize in the forms I,[56] II,[54,57] and III[58] of iPB, respectively. Reproduced with permission from Ref. [1]. Copyright 2014 by Wiley & Sons

to a relative energy minimum with values of the torsion angles θ_1 and θ_2 slightly deviated from the exact *trans* (180°) and *gauche* (60°) values typical of the 3/1 helix. According to this calculations form I is the most thermodynamically stable form, whereas form II and form III are metastable forms.

Models of the crystal structures of forms I, II, and III of iPB are shown in Figures 4–6, respectively. In the structure of form I (Figure 4), six chains (right-handed and left-handed helices) are included in the unit cell, giving a high crystal density of ρ_c = 0.95 g/cm^3 and a rather high melting temperature of 130°C.[41] The crystal structure of form I of iPB (Figure 4) is a prototype of the class of polymer crystals whose crystallization is guided by the entropic *principle of conservation of the chain symmetry*,[1] which establishes that *a molecule in a crystal tends to maintain part of its symmetry elements, provided that this does not cause a serious loss of density*.[1,3,5] According to this principle, as shown in Figure 4 for form I of iPB,[31] the local 3/1 helical axes of the molecules are maintained in the crystal lattice and coincide with the crystallographic 3-fold axes.

The crystal structure of form II of Figure 5[33–37] is a typical example of the tetragonal packing of chains in helical conformation **s**(*M*/*N*) with complex helical symmetry characterized by non integer ratio *M*/*N*. However, it is characterized by a low crystal density of ρ_c = 0.907 g/cm^3, which is lower than that of form I (ρ_c = 0.95 g/cm^3) and only slightly higher than that of the amorphous state (ρ_a = 0.868 g/cm^3). The melting temperature of form II is about 120°C, lower than that of form I.[41,42]

The structure of form III of iPB of Figure 6[38] is a typical example of symmetry breaking,[1] because the 4/1 helical symmetry of the chains is not a crystallographic symmetry and is lost in the crystals (Figure 6). The crystal density of form III is lower than that of form I and is similar to that of form II with a melting temperature of 100°C-105°C,[41,42] lower than that of form II. The structure of form III of iPB is also an example of chiral packing even though the polymer is achiral.[1,5] In the structure of Figure 6, indeed, helical chains with the same chirality (right-handed or left-handed) are included in the unit cell resulting in an isochiral packing. This is the case of *chiral but racemic* polymers,[1,5,8] as all isotactic poly(α-olefins) where the monomeric unit presents a stereoisomeric center, which is not a true asymmetric carbon.[46–48] In the structure of form III of iPB the space group is chiral but the polymer is, of course, nonchiral because the chirality of the unit cell is compensate by the presence of equal fractions of crystals of the enantiomorphous space groups, characterized by units cells containing only right-handed and only left-handed helices, as in the case of the intercrystallite optical compensation forming a *conglomerates*.[8,49–52]

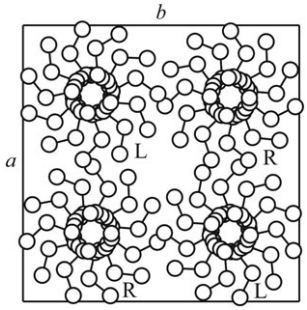

FIGURE 5 Model of packing of form II of iPB with chains in 11/3 helical conformation packed in a tetragonal unit cell according to the space group $P\bar{4}$.[33–37] R and L indicate right-handed and left-handed helices, respectively

According to the higher density and melting temperature, form I is the most stable form of iPB. However, the tetragonal form II is the kinetically favored modification of iPB and is generally obtained by crystallization from the melt.[33,35,41,53–59] Form II is metastable and spontaneously transforms into the most stable form I on storage at room temperature.[31,41,53–65] Form III is also metastable and is generally obtained by crystallization form dilute solutions.[41–43] It also transforms spontaneously into the stable form I on drawing.

The form I-form II polymorphism of iPB is a typical monotropic polymorphism defined by the free-energy plot of Figure 1A. Form I has the lowest free energy at all temperatures below its melting temperature, and, therefore, is the thermodynamically most stable crystal structure at all temperatures. Form II is a metastable polymorphic form that melts at temperature T_{mII} lower than the melting temperature of form I (T_{mI}). Therefore, a crystal-crystal transformation

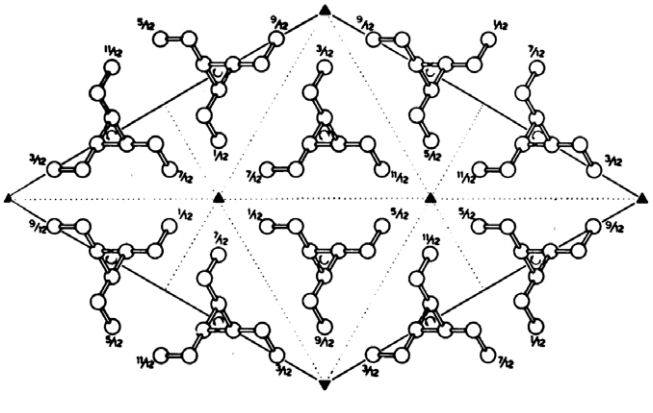

FIGURE 4 Model of packing of the form I of iPB,[31] with chains in 3/1 helical conformation packed in a trigonal lattice according to the space groups *R*3*c* or $R\bar{3}c$. Reproduced with permission from Ref. [31]. Copyright 1960 by Nicola Zanichelli Ed

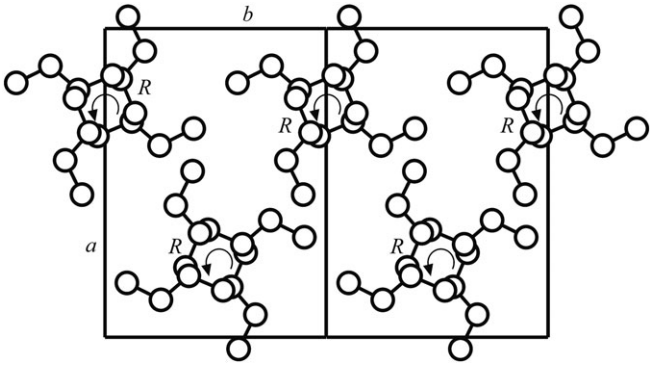

FIGURE 6 Model of packing for the crystal structure of form III of iPB[38] with chains in 4/1 helical conformation packed in an orthorhombic unit cell according to the space group $P2_12_12_1$. *R* and *L* indicate right-handed and left-handed helices, respectively. Reproduced with permission from Ref. [1]. Copyright 2014 by Wiley & Sons

between the forms I and II does not occur with temperature. However, the metastable high energy form II always crystallizes from the melt of iPB, by simple cooling from the melt to room temperature or by isothermal crystallizations, and then spontaneously transforms into the more stable form I by a crystal-crystal transformation at room temperature.[31,41,53–65] The polymorphic transformation occurs over a wide temperature range, from the glass transition temperature (−25°C) up to 100°C[63–65] with a maximum rate at around 20°C.[65–67] At this temperature, completion of the transformation requires several days.[63,66,68] The transformation of form II into form I is irreversible and the initial crystal form II can be obtained only by remelting the sample (monotropic polymorphism).

Therefore, in normal conditions of crystallization, form II is obtained by melt-crystallization and form I is obtained from form II by crystal-crystal transformation at room temperature. As shown in Figure 2, for systems involving other intensive variables, such as pressure, stress, and composition of a mixture, the free energy surfaces of the individual phases are treated in a similar manner but the crystallization pathways may be altered. In the case of iPB, and under particular conditions, such as pressure), crystals of form I melting at very low temperatures of 90°C-95°C can be obtained by direct crystallization from the melt.[42,68–76] Crystals of form I obtained from transformation of form II generally melt at much higher temperature (130°C). Because of the lower melting temperature, this form I crystallized directly from the melt has been defined form I′ and has been regarded as a defective form I, having the same crystal structure of Figure 4 but with crystals with much smaller thickness.[42,68,69]

The physical properties of iPB are greatly affected by the spontaneous form II-form I transformation because of the increase of density, melting temperature, and mechanical strength.[30,41,53,64,65,77,78] The transformation is rather slow and is complete only after days or weeks at room temperature.[41,53,63–65,67,75–82] The kinetics of this solid state transition depends on the aging temperature and on the molecular structure, in particular, the molecular mass,[43,55,63] the stereoregularity,[55,63] and the presence of comonomer units.[34,63,83] The kinetics is also accelerated by application of pressures[75,76] and shear or tensile stresses.[81,84,85]

Models of the mechanism of the spontaneous form II-form I transformation have been proposed based, in particular, on data of electron diffraction patterns on single crystals recorded during the transformation of form II and of those of crystals of form I′ obtained by direct crystallization form the melt.[60–62,76] Studies on the transformed form I crystals lying flat-on illustrated a "twinned" orientation of the transformed form I crystals, which differs from that of the directly formed form I′. Electron diffraction patterns of iPB taken during the phase transition, that is, before the complete transformation of the form II crystals contain one diffraction set of the original form II and two sets of the twinned form I crystals.[61,76] A careful analysis of the superimposed electron diffraction patterns indicates that the original form II and the transformed form I exhibit common (110) lattice planes.[61,76] An explanation of this twinned structure was then first proposed by Holland and Miller.[42] They related the twinned orientation of transformed form I to the existence of growth sectors of the parent crystals of form II. It was suggested that the different sectors of the tetragonal crystal of form II, which exhibit different folding directions, give two differently oriented crystals of form I resulting in two sets of diffraction spots of the transformed form I.[42] However, experimental results that two orientations of form I crystals within a single growth sector of form II were also obtained, and only one form I crystal orientation was created in different sectors of the original form II crystal,[44,61] do not support this model of transformation.

Based on all these experimental results, a rational explanation of the form II-form I transition has been proposed with full consideration of conformational and steric constraints.[61,62] In particular, the spontaneous transformation of form II into form I illustrates the constraints set by preservation of the helical chirality.[62] The structural aspect of the transformation is schematically presented in Figure 7. The tetragonal structure of form II (Figures 5 and 7A) is characterized by alternation of the helical chirality of the 11/3 helical chains along both *a* and *b* axes of the unit cell. As a result, the (110) planes are made of isochiral helices (R or L), with the successive layers (the 220 planes) made of isochiral chains of opposite chirality (Figures 5 and 7A). The trigonal form I is also characterized by layers parallel to the (110) planes containing chains in 3/1 helical conformation having the same chirality (R or L, Figures 4 and 7C) with alternation of layers containing isochiral chains of opposite chirality. Upon transformation, it is observed that the (110) planes of the resultant trigonal unit cell are parallel to the (110) planes of the parent tetragonal unit cell (Figure 7).[57,61] This relative orientation illustrates the requirement of preservation of the helical hands in the transformation. In fact, any other relative orientation of initial and final lattices would require reversal of helical hands of at least a fraction of the stems. In addition, the transformation is facilitated by a very fortunate near-matching (−5%) of interhelical distances in the two planes, which means that helix shifts are minimized during the transformation. However, the contraction is nearly 20% in the orthogonal direction, with resultant development of cracks in the transformed crystal.[61] Furthermore, this transformation is characterized by the existence of a geometrical favorable "invariant plane," which also meets the preservation of the helix chirality requirement.[62] In particular, the transformation proceeds across growth sector boundaries, which exist in single crystals following crystallographic constraints, which are much more important than the fold-orientation requirement.

The mechanism of this solid-to-solid phase transition from form II to form I is, therefore, the cooperative occurrence of chain conformational change and packing mode change, so that the energy barrier to cross becomes as low as possible which can explain the formation of the twin structure of form I crystals.[86] These movements result in a transient structure that accounts for the diffraction pattern observed during transformation.[87] The transformation takes place by cooperative movement of right-handed (R) and left-handed (L) chains in form II, such as to form pairs of enantiomorphic helices as in the structure of form I (Figure 7C).[86] In form I these pairs are arranged in a hexagonal packing mode and orient along the^{110} direction. Conversely, the R and L chains in the form II crystal are arranged in a zigzag mode along the^{110} direction. The pairs of R and L helices similar to that of form I can be simply produced by the opposite side movement of the helices.[86]

Detailed studies of the kinetics of form II-form I transformation and of the dependence of the transformation rate on the aging temperature

and time have revealed that this solid-solid transition is a two-step process including nucleation and growth.[88] This was suggested by the results of experiments of isothermal crystallization of iPB in form II followed by successive annealing at a lower temperature (T_l) and at a higher temperature (T_h) to promote transition from form II to I,[88] compared with simple aging at a single temperature (T_s). In fact, in these experiments it has been observed that more form I is obtained after being annealed at T_l and T_h than annealed at a single aging temperature

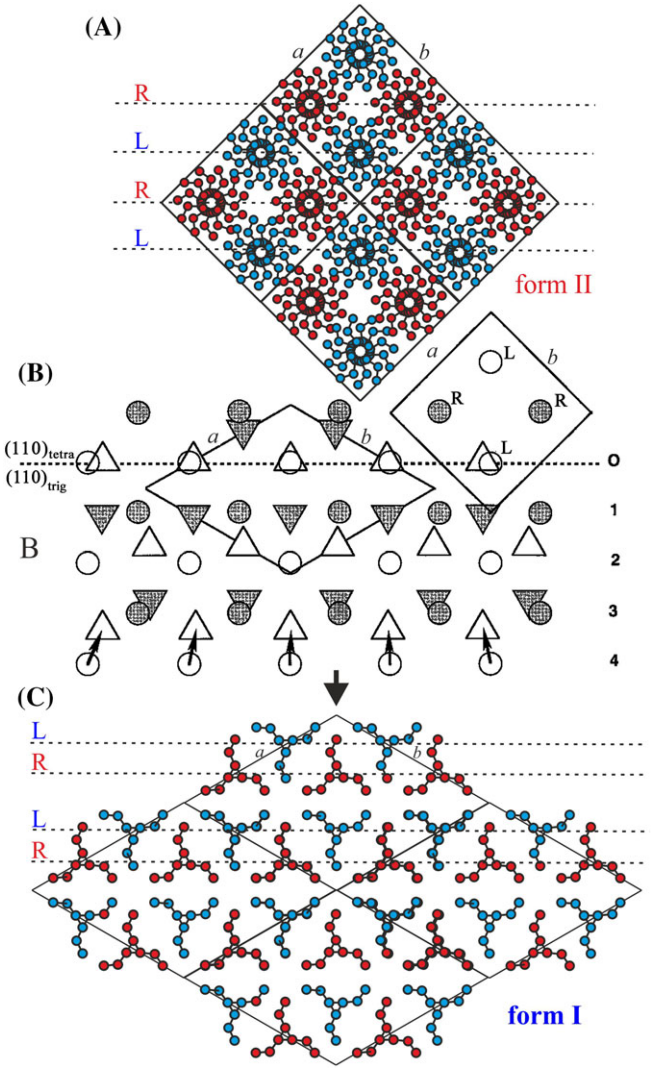

FIGURE 7 Scheme of the mechanism of solid-solid transformation of the tetragonal form II of iPB into the trigonal form I. Chains of forms II and I in 11/3 and 3/1 helical conformations, respectively, of different chirality, right-handed (R) and left-handed (L), are indicated in red and blue, respectively, in (A) and (C). In (B) the chains of the two forms in 11/3 and 3/1 helical conformations are represented as circles (for the 11/3 helix of the tetragonal form II) and triangles (for the 3/1 helix of the trigonal form I), and by the light and shaded symbols for chains of different chirality. The "invariant plane" is $(110)_{tetra}$ for the tetragonal form II and $(110)_{trig}$ for the trigonal form I. The transformation is initiated in layer 0 and takes place with limited lateral movements of chains, and propagates both sideways and downward. As the transformation proceeds to planes 1, 2, 3, ..., movements (illustrated in plane 4) are amplified because of the nearly 20% densification upon transformation, but the helical hands are maintained in the process[61,62] Adapted from Ref. [61] and reproduced with permission from Ref. [62]. Copyright 1998 by American Chemical Society

T_s for the same period of time.[88] Annealing at low temperature T_l benefits nucleation due to internal stress induced by unbalanced shrinkage of amorphous and crystalline phases because of their different thermal expansion coefficients, while annealing at higher T_h is beneficial to growth owing to rapid segmental diffusion at that temperature.[88] Both nucleation and growth rates as a function of temperature showed a Gaussian distribution with maxima at −10°C and 40°C, respectively, corresponding to the optimum temperatures of nucleation and growth, respectively.[88] Moreover, the transition rate was increased with the increase of crystallization temperature due to higher internal stress built up during cooling down from higher crystallization temperature to the nucleation temperature T_l. These results allow separating the form II-form I polymorphic transition into nucleation and growth providing a simple and effective way for rapid transition of form II to I in iPB.[88]

As already mentioned, besides intensive external parameters that define the condition of crystallization, molecular parameters, as the presence of molecular defects, may define the diagrams of Figure 1 and alter the crystallization pathways. In particular, the presence of constitutional defects, as comonomeric units, or of defects of stereoregularity may influence both the thermodynamic stabilities of form I and form II and the kinetics of crystallization from the melt. Two different situations are worth mentioning. Defects may increase the thermodynamic stability of form II and decrease that of form I. With reference to the scheme of Figure 1A, the free energy curves of forms I and II are inverted and form II becomes the thermodynamically more stable form and the kinetically favored polymorphic form. In this situation, form II crystallizes from the melt and does not transform into form I by aging at room temperature. A second situation is when defects increase the kinetics of melt crystallization of form I and contemporarily decrease the thermodynamic stability of form II. In this case, the free energy curve of form II becomes too high at any temperature and the kinetics of crystallization of form I and form II become competitive, resulting in the direct crystallization of form I from the melt. The first case has been observed in copolymers of iPB with linear α-olefins with number of carbon atoms higher than 5 and branched comonomers.[34] In this copolymers the transition of form II into form I is greatly retarded or form II is completely stabilized.[34,35] The second case has been observed in stereodefective iPB samples, where the presence of stereodefects allows direct crystallization of form I from the melt because of the increase of the kinetics of melt crystallization of form I and the decrease of the thermodynamic stability of form II.[28,29]

2.1 | Influence of stereodefects on the polymorphism of iPB

The discovery of soluble organometallic catalysts for the polymerization of olefins has allowed production of new polyolefins having molecular structures that cannot be obtained with conventional Ziegler-Natta catalysts.[89] These catalysts allow controlling the concentration of *stereo* and *regio*-defects and uniform placement of constitutional defects, as comonomeric units, along the chains,[89] with important consequences on the physical and mechanical properties. For example, in the case of isotactic[21–23] and syndiotactic polypropylene[24–26] this synthetic strategy has allowed tailoring the physical properties of the materials by controlling the crystallization behavior.[21–26]

Also for iPB, different samples characterized by macromolecules containing controlled and different concentrations of regio-irregularities and stereo-irregularities and different molecular masses have been synthesized using different organometallic catalysts.[27] The random distribution of defects and the presence of a single type of defect (stereodefects or regiodefects) has allowed the study of the influence of a specific molecular defect and of the molecular mass on the crystallization of form I and form II of iPB. It has been demonstrated that the controlled incorporation of stereodefects influences the crystallization behavior with remarkable consequences in term of physical properties and practical interest of iPB.[28–30] In particular, samples of iPB of different stereoregularity, containing one type of stereoirregularity, *rr* triad defects, have been prepared with the metallocene catalysts of Figure 8.[27] Depending on the structure of the catalyst, the concentration of *rr* defects in the polymer has been varied between 0.3% and 5%, and the corresponding melting temperatures of the iPB samples varies in the range 125°C-70°C.[27]

The X-ray diffraction profiles of the iPB samples crystallized from the melt by cooling the melt to room temperature at 2.5°C/min, and of the same samples kept at room temperature for 1 month are reported in Figure 9A,B, respectively.[28,29] The more stereoregular samples with concentration of *rr* stereodefects lower than 1.4 mol% show the usual behavior and crystallize from the melt into form II, as indicated by the presence of the $(200)_{II}$, $(220)_{II}$, and $(213)_{II}$ + $(311)_{II}$ reflections at 2θ = 11.9, 16.9, and 18.3°, respectively, in the diffraction profiles a-d of Figure 9A.[28,29] Less stereoregular samples crystallize from the melt, instead, in the stable form I,[28,29] as indicated by the presence of $(110)_{I}$, $(300)_{I}$, and $(220)_{I}$ + $(211)_{I}$ reflections of form I at 2θ = 9.9, 17.3, and 20.5°, respectively, in the diffraction profiles e-h of Figure 9A.[28,29] The presence of *rr* stereodefects in concentration higher than 2 mol%, induces the crystallization from the melt of form I instead of the metastable form II.[28,29]

As discussed above, crystals of form I obtained by direct crystallization from melt in stereoirregular iPB samples of Figure 9A (profiles e-h) correspond to the form I′. This was the first experimental evidence of the crystallization of the stable trigonal form I of iPB directly from the melt at atmospheric pressure.[28,29]

Figure 9B shows that crystals of form II obtained from the melt in the more stereoregular samples (profiles a-d of Figure 9A) transforms into form I upon aging at room temperature (profiles a-d of Figure 9B), whereas in the streoirregular samples crystallized in form I′ (profiles e-h of Figure 9A) no phase transition is observed upon aging (profiles e-h of Figure 9B).[28,29]

The data of Figure 9 correspond to crystallization from the melt at low cooling rate of 2.5°C/min. The effect of the cooling rate on the crystallization of form I (form I′) and form II is shown in Figure 10.[29] The diffraction profiles of Figure 10 show that the most stereoregular sample crystallizes in the form II at any cooling rate (Figure 10A), whereas the more stereodefective samples crystallize as mixtures of form I′ and form II, and the amount of form I′ increases with decreasing cooling rate (Figure 10B,C). The most irregular sample iPB9 crystallizes from the melt at cooling rate of 2.5°C/min almost completely into form I′ (Figure 10D).

The crystallization of forms I and II upon cooling from the melt also depends on the molecular mass.[29] In the case of stereoirregular samples the amount of form I′ increases with the decrease of molecular mass and in samples with high molecular mass the crystallization of high amount of form II has been observed even at low cooling rate of 2.5°C/min.[29] Moreover, for stereoregular samples with low molecular mass a small amount of crystals of form I′ has been observed upon melt crystallization at the highest cooling rate.[29]

The conclusion that in stereodefective iPB samples crystals of form I are obtained directly from the melt and not from rapid transformation of form II eventually formed at the early stage of crystallization, has been demonstrated by experiments of time resolved X-ray diffraction during crystallization.[28,29] Figure 11 shows the data for the sample iPB**6** with [*rr*] = 2.8%.[28] The diffraction profiles have been recorded during the isothermal crystallization only in the range 2θ = 8-14°, where the $(110)_{I}$ reflection of form I at 2θ = 9.9° and $(200)_{II}$ reflection of form II at 2θ = 11.9° occur. The diffraction pattern of the melt has been first recorded at 180°C (profile a of Figure 11B). The samples has been cooled to the crystallization temperatures T_{c1} = 55°C and T_c = 25°C (Figure 11A), and the diffraction profiles have been recorded at T_{c1} (Figure 11C) and at T_c = 25°C (Figure 11D).

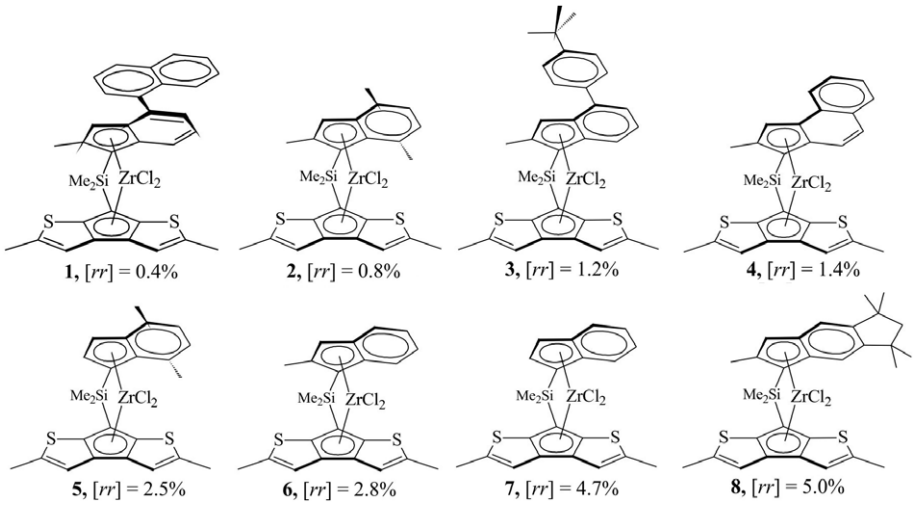

FIGURE 8 Structures of the zirconocene catalysts used for the synthesis of samples of iPB having different stereoregularity. [27] Each catalyst produces the indicated concentration of the *rr* defects

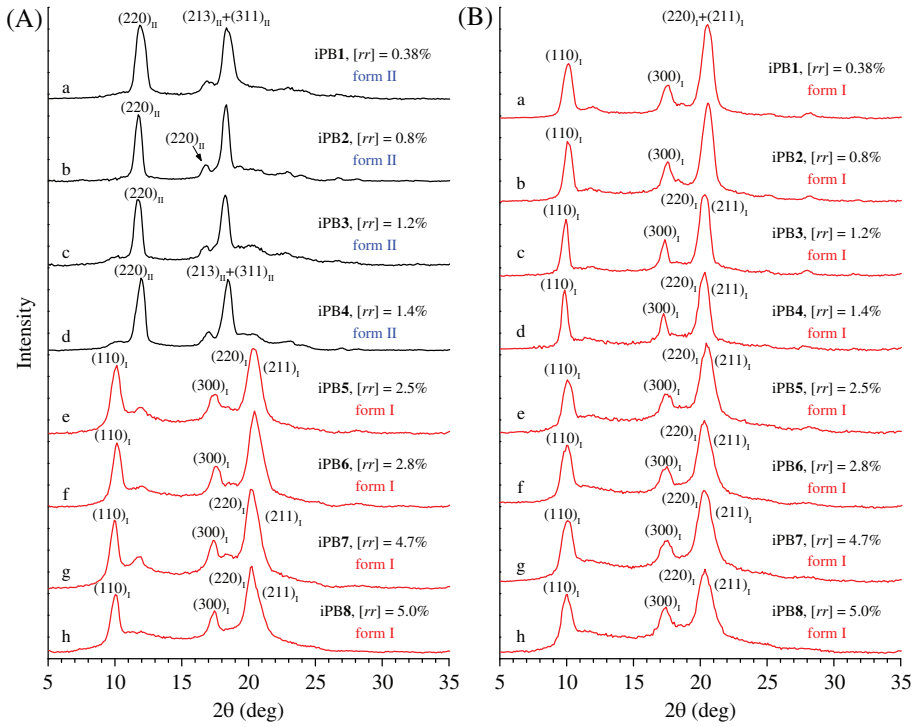

FIGURE 9 X-ray diffraction profiles of iPB samples having different concentrations of *rr* stereodefects crystallized by cooling the melt at cooling rate of 2.5°C/min (A) and of the same samples kept at room temperature for at least 1 month (B).[28] Reproduced with permission from Ref. [28]. Copyright 2008 by Wiley VCH

Figure 11B clearly indicates that the sample iPB**6** crystallizes from the melt by cooling to −30°C in form I (profile b of Figure 11B). The diffraction profiles recorded at 55°C and at 25°C during the isothermal crystallization at 55°C of Figure 11C and at 25°C of Figure 11D show that, starting from the amorphous halo of the melt, the $(110)_I$ reflection of form I at 2θ = 9.9° appears at the beginning of the crystallization (5 minutes) and its intensity increases during crystallization, when the $(200)_{II}$ at 2θ = 11.9° of form II is never observed.[28] This indicates that for this stereoirregular sample form I crystallizes directly from the melt.[28,29]

The direct crystallization of form I from the melt in stereoirregular samples of iPB has been observed even when the samples crystallize in mixtures of form I and form II,[28,29] as in the case of samples of Figures 10B,C, where the amount of form I′ in the mixtures increases with decreasing cooling rate, that is, in conditions of slow crystallization. Also in isothermal crystallizations from the melt mixtures of forms I and II are obtained and the amount of form I is dependent on the crystallization temperature. Examples are shown in Figures 12 and 13 for the more isotactic sample iPB3 with [*rr*] = 1.2% and for the more stereoirregular sample iPB7 with [*rr*] = 4.7%.

The DSC curves of the samples iPB3 and iPB7 cooled from the melt to −30°C at cooling rate of 2.5°C/min are shown in Figures 12A and 13A. In the crystallization experiments, after melting at 180°C (Figures 12B and 13B), the diffraction profiles have been recorded during isothermal crystallization at the temperatures T_{c1} = 70°C and T_c = 60°C, 40°C, and 25°C for the sample iPB3 (Figure 12C-F) and T_c = 60°C, 50°C, and 25°C for the sample iPB7 (Figure 13C-F). The more isotactic sample iPB3 crystallize by cooling the melt to −30°C essentially in the form II, as indicated by the diffraction profile c of Figure 9A. The diffraction profiles of Figure 12C,D recorded at 70°C and 60°C, respectively, during the isothermal crystallizations at 70°C and 60°C of the sample iPB3 clearly show that the $(200)_{II}$ reflection at 2θ = 11.9° of form II appears at the beginning of the crystallization, when the $(110)_I$ reflection of form I at 2θ = 9.9° is not observed. The intensity of the $(200)_{II}$ reflection of form II increases during the crystallization and the $(110)_I$ reflection of form I appears after 5 minutes from the beginning of the crystallization (Figure 12C,D). Therefore, also in this case crystals of form I are obtained by crystallization from the melt, along with crystals of form II, and not from the transformation of crystals form II. On the other hand at high temperatures of 60°C-70°C the transformation of form II into form I is very slow, and crystals of form II obtained at 60°C and 70°C remain stable till the sample is maintained at the crystallization temperature. At lower crystallization temperatures of 40°C and 25°C the crystallization is faster (Figure 12E,F) and the $(200)_{II}$ and $(110)_I$ reflections of forms II and I, respectively, appear at the beginning of the crystallization but the sample still crystallize mostly in form II, the intensity of the $(110)_I$ reflection of form I at 2θ = 9.9° being always very low. Also at these low temperatures form I crystallizes from the melt, in these cases contemporarily to form II.

The more irregular sample iPB**7** with [*rr*] = 4.7 mol% crystallizes from the melt completely in the stable form I by cooling the melt to −30°C at low cooling rates (eg, 2.5°C/min), as indicated by the diffraction profile g of Figure 9A that presents only the $(110)_I$, $(300)_I$, and $(220)_I$ + $(211)_I$ reflections of form I at 2θ = 9.9, 17.3, and 20.5°, respectively, or in isothermal melt-crystallizations performed at high crystallization temperatures (Figure 13C,D). However, this sample crystallizes from the melt in mixtures of forms I and II at high cooling

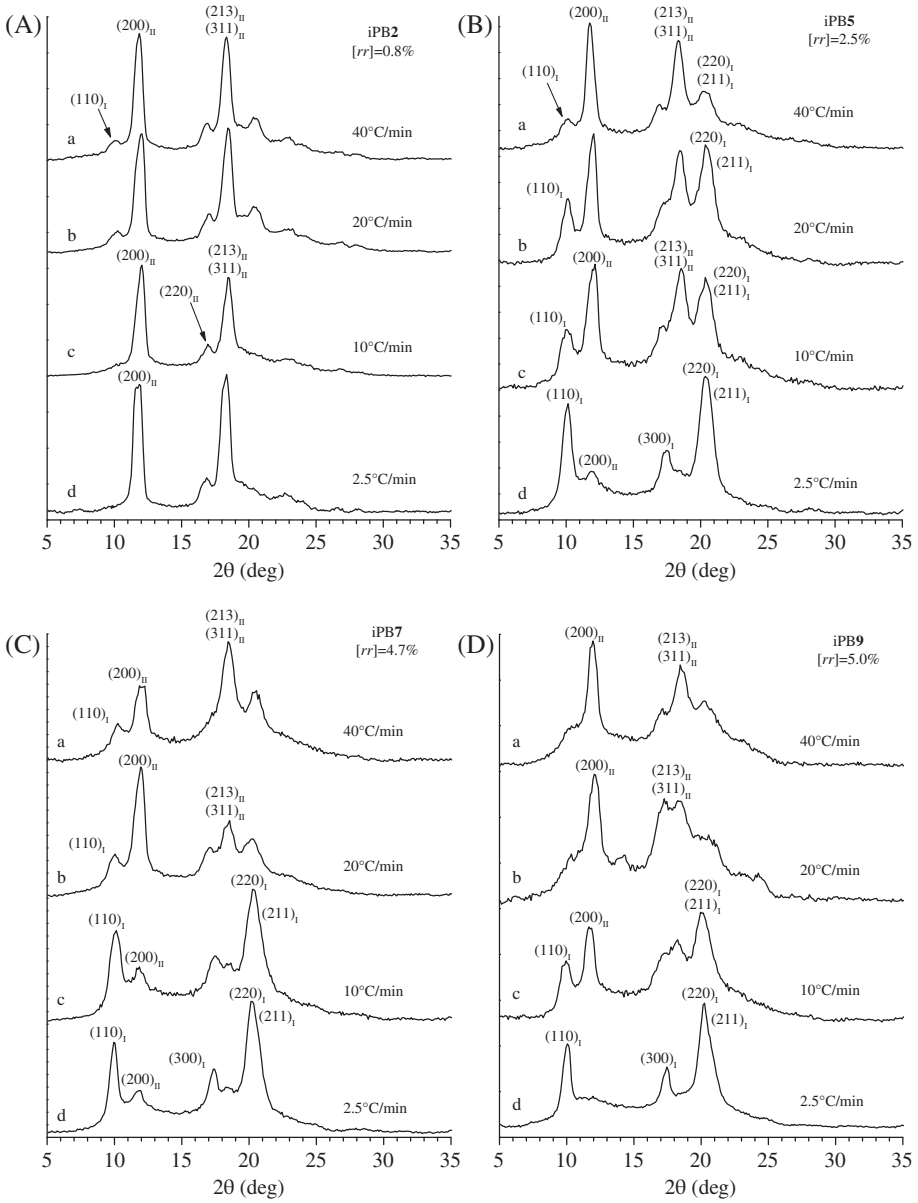

FIGURE 10 X-ray diffraction profiles of stereodefective iPB samples crystallized from the melt by cooling the melt at the indicated different cooling rates.[29] Reproduced with permission from Ref. [29]. Copyright 2009 by American Chemical Society

rates or in isothermal melt-crystallizations at low crystallization temperatures (Figure 13E,F). The diffraction profiles recorded at 70°C and 60°C, during the crystallization at 70°C and 60°C of Figure 13C,D, respectively, clearly show that, starting from the amorphous halo of the melt, the $(110)_I$ reflection of form I at $2\theta = 9.9°$ appears after 15 minutes at 70°C (Figure 13C) and 10 minutes at 60°C (Figure 13D), when the $(200)_{II}$ reflection at $2\theta = 11.9°$ of form II is not observed. The intensity of the $(110)_I$ reflection of form I increases during the crystallization and the $(200)_{II}$ reflection of form II at $2\theta = 11.9°$ never appears at 70°C (Figure 13C). At 60°C a small peak corresponding to the $(200)_{II}$ reflection of form II appears only at longer crystallization time, after about 30 minutes (Figure 13D).[28,29]

At lower crystallization temperatures of 50°C and 25°C the sample iPB**7** crystallizes in mixtures of crystals of forms I and II, as indicated by the presence of both $(110)_I$ and $(200)_{II}$ reflections of forms I and II in the diffraction profiles of Figures 13E,F. At 50°C, starting from the amorphous halo of the melt the $(110)_I$ reflection of form I at $2\theta = 9.9°$ appears at the beginning of the crystallization, after 10 minutes, whereas the $(200)_{II}$ reflection of form II at $2\theta = 11.9°$ is still absent (Figure 13E). The intensity of the $(110)_I$ reflection of form I increases during the crystallization at 50°C and the $(200)_{II}$ reflection of form II appears only at longer crystallization time, at least after 15 minutes from the beginning of the crystallization (Figure 13E). At the end of the crystallization at 50°C the $(200)_{II}$ and $(110)_I$ reflections of forms II and I have nearly the same intensity. At the crystallization temperature of 25°C (Figure 13F) the $(110)_I$ and $(200)_{II}$ reflections of forms I and II appears about contemporarily at the beginning of the crystallization. The slightly higher intensity of the $(110)_I$ reflection of form I than that of the $(200)_{II}$ reflection of form II at crystallization time of 10 minutes (Figure 13F), indicates that crystals of form I probably crystallize before those of form II. The intensities of $(110)_I$ and $(200)_{II}$ reflections of forms I and II increase during the crystallization at

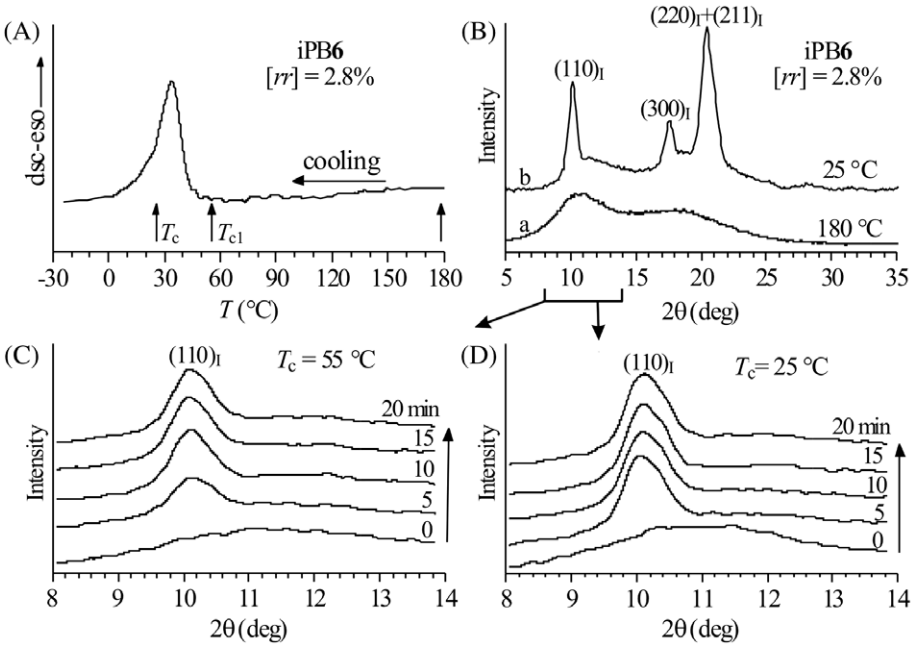

FIGURE 11 (A) DSC cooling curve from the melt at 2.5°C/min, and (B) X-ray diffraction profiles recorded at 180°C in the melt and at 25°C after cooling from 180°C of the sample iPB**6** with [*rr*] = 2.8 mol%. (C,D) X-ray diffraction profiles recorded in the range 2θ = 8-14° at the crystallization temperatures of 55°C (C) and 25°C (D) during the isothermal melt-crystallization.[28]
Reproduced with permission from Ref. [28]. Copyright 2009 by Wiley VCH

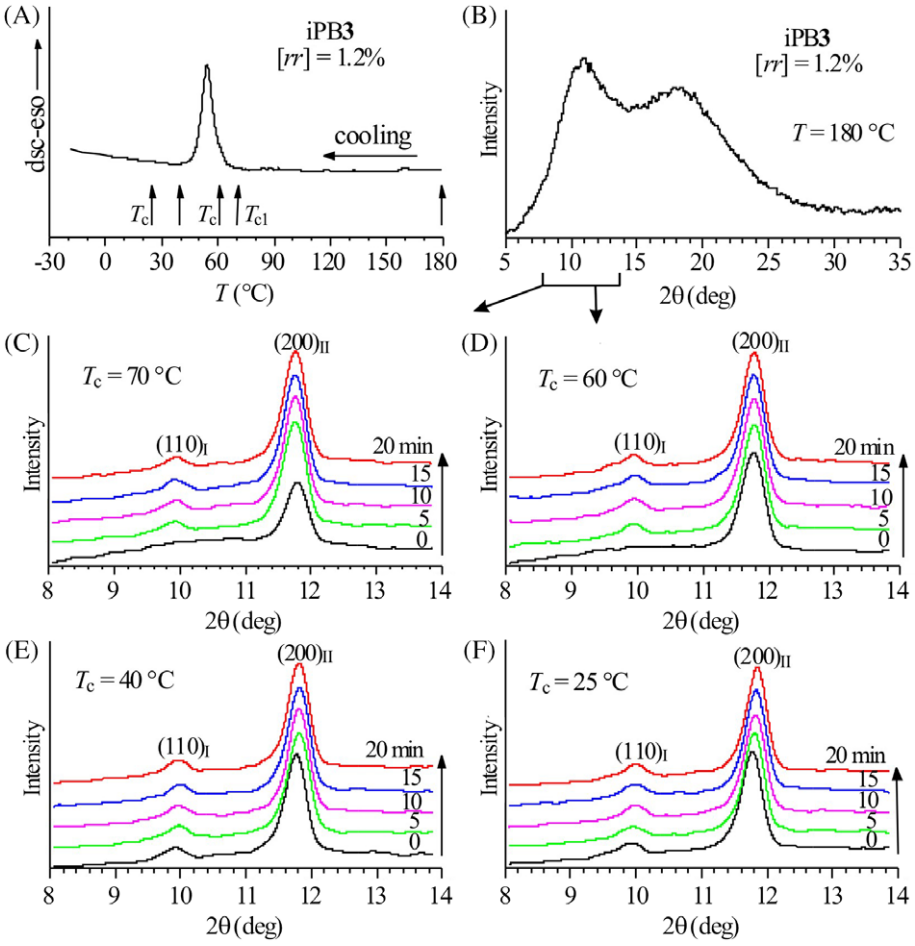

FIGURE 12 (A) DSC cooling curve from the melt at 2.5°C/min and (B) X-ray diffraction profile recorded at 180°C in the melt of the sample iPB**3** with [*rr*] = 1.2 mol%. (C-F) X-ray diffraction profiles recorded at the crystallization temperatures of 70°C (C), 60°C (D), 40°C (E), and 25°C (F) during the isothermal crystallizations from the melt.[28]

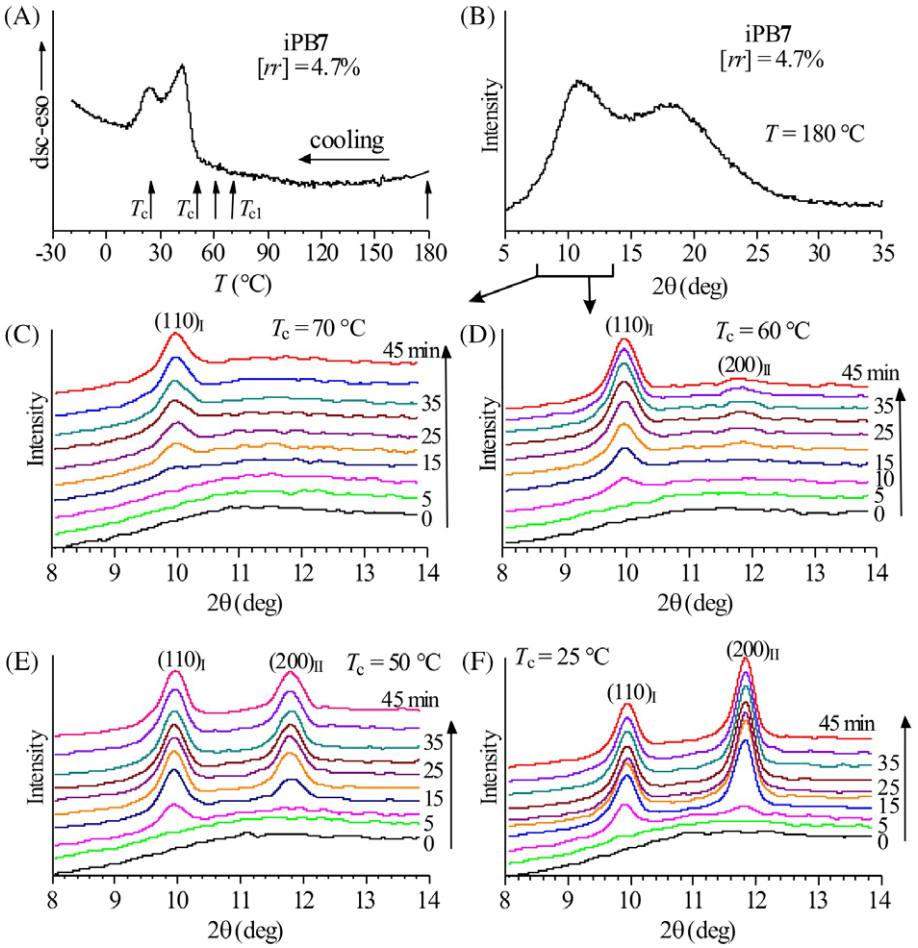

FIGURE 13 (A) DSC cooling curve from the melt at 2.5°C/min and (B) X-ray diffraction profile recorded at 180°C in the melt of the sample iPB7 with [*rr*] = 4.7 mol%. (C-F) X-ray diffraction profiles recorded at the crystallization temperatures of 70°C (C), 60°C (D), 50°C (E), and 25°C (F) during the isothermal crystallizations from the melt.[28]

25°C, and at the end of the crystallization the intensity of the $(200)_{II}$ reflection of form II at 2θ = 11.9° becomes higher than that of the $(110)_{I}$ reflection of form I, indicating that higher amount of form II crystallizes at 25°C, when the crystallization is fast.[28]

The data of Figures 9–13 indicates that the modification of the molecular structure of iPB through the controlled introduction of defects of isotacticity allows the crystallization of the stable form I′ from the melt instead of the kinetically favored form II. The *rr* triad defects play a double role. On one hand, the kinetics of crystallization of form I is improved because of the increased flexibility of the chains, so that crystallizations of forms I and II become competitive,[29] as shown by the simultaneous crystallization of the two polymorphs in Figures 11 and 13. On the other hand, the incorporation of *rr* defects reduces the thermodynamic stability of the 11/3 helix and of form II, whereas no great effect is expected for the 3/1 helix.[29] This results in the preferential crystallization of form I′ in conditions of slow crystallizations, as slow cooling or high crystallization temperatures. Low molecular masses play a similar role in improving the crystallization kinetics of form I in low isotactic samples through the increased mobility of the chains. This effect is less important is highly isotactic samples for which form II has still a reasonable stability and remains the kinetically favored polymorph.[29]

The opposite results of Figure 10A that crystallization of form I′ in more isotactic samples is favored at high cooling rates has been explained on the basis of stability and number of nuclei of forms I and II that must form and grow at the crystallization temperature.[29] The values of the minimum lamellar thickness necessary to allow growing of crystals of forms I and II at a given crystallization temperature[29] have been determined from the data of crystallization temperature T_c, evaluated by DSC cooling scans at rates of 2.5, 10, 20, and 40°C/min (shown in Figure 14A), using the Gibbs-Thomson equation:[90,91]

$$l_{min} = \frac{2\sigma_e T_m^0}{\Delta H_m \Delta T}$$

where ΔH_m is the melting enthalpy per unit volume of the crystal phase, σ_e is the end-surface free energy per unit area of polymer crystals[75] and $\Delta T = T_m^0 - T_c$ is the undercooling with T_m^0 the equilibrium melting temperature of the polymorphic form. Figure 14B shows that the values of minimum size of lamellae l_{min} increases with the increase of the crystallization temperature T_c (decreasing undercooling), and the minimum thickness necessary to allow growing of crystals is higher for form II than for form I′.[29] However, in highly isotactic samples and in normal crystallization conditions only form II crystallizes from the melt because of the much higher crystallization rate of form II.[75] In the

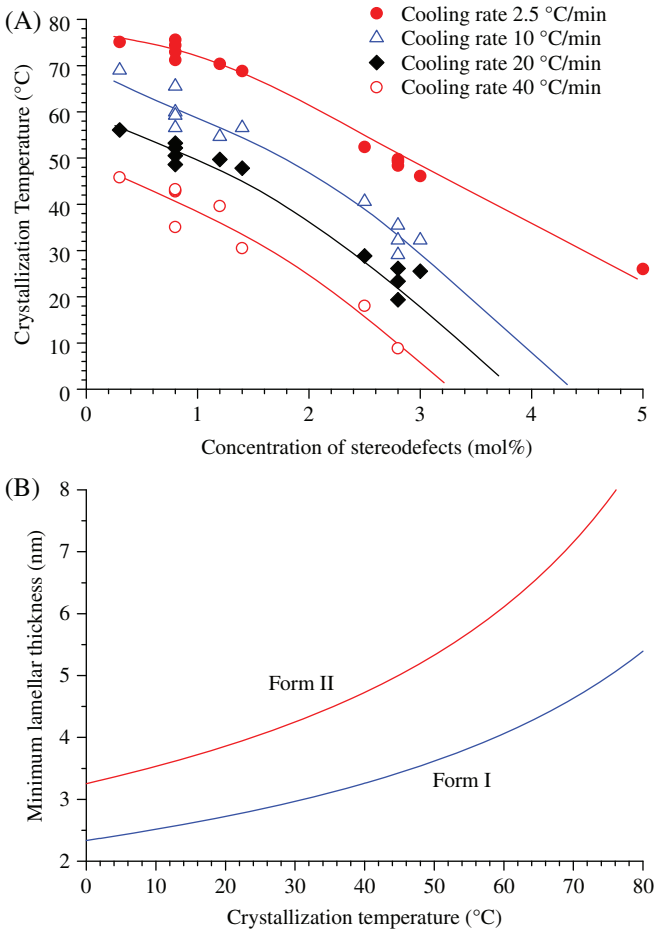

FIGURE 14 (A) Values of crystallization temperatures of samples of iPB of different stereoregularity determined by the exothermic peaks in DSC thermograms recorded during cooling at 2.5°C/min (●), 10°C/min (△), 20°C/min (◆), and 40°C/min (○). The different points at the same stereodefect concentration of 0.8 and 2.8 mol% correspond to samples having different molecular mass[29]. (B) Values of the minimum lamellar thickness necessary to allow growing of crystals of form I and form II vs the crystallization temperature.[29]

presence of even a small concentration of *rr* stereodefects, the crystallization kinetics of form I is improved and a reasonable number of nuclei having thickness higher than l_{min} can form upon cooling. For these samples, with amount of *rr* defects lower than 1.4 mol%, the amount of crystals of form I′ increases with the increase of the cooling rate (Figure 10A) because the minimum lamellar thickness l_{min} decreases with the decrease of the crystallization temperature T_c (Figure 14B), which decreases with the increase of cooling rate (Figure 14A).[29]

The change of the crystallization pathway of Figure 1A and of the monotropic polymorphism of iPB upon introduction of *rr* defects of stereoregularity with the crystallization of the stable form I from the melt has also relevant consequences on the physical and mechanical properties of iPB.[28,30] The stress-strain curves of the samples iPB**2** and iPB**6** with 0.8 and 2.8 mol% of *rr* defects, respectively, melt-crystallized and aged for 1 month are shown in Figure 15.[28,30] For the more isotactic sample iPB**2**, the aging allows transition of form II, crystallized from the melt, into form I. Correspondingly, this phase transformation produces a significant modification of the mechanical properties (Figure 15A), with increase of values of modulus and of yield stress (as occurs in iPB samples prepared with Ziegler-Natta catalysts).[28,30] For the stereoirregular sample iPB**6** that crystallize in form I′ from the melt, no polymorphic transformation occurs during aging at room temperature and, correspondingly, the mechanical properties do not change during aging at room temperature (Figure 15B).[28,30]

2.2 | Influence of constitutional defects: Copolymers of iPB

Studies on the crystallization behavior of copolymers of iPB with different comonomeric units prepared with Ziegler-Natta catalysts have been extensively reported in the old literature[34,63,83] and in more recent papers.[92,93] These studies have shown that comonomeric units having different size influences differently the crystallization behavior and the rate of the form II-form I transformation.[34] In particular, ethylene counits accelerate the transition, whereas longer 1-olefins or crowded 1-olefins stabilize form II that no longer transforms into form I.[34]

However, as these copolymers were prepared with Ziegler-Natta catalysts, their molecular structure is complex because of the non uniform and nonstatistical distribution of comonomers and other defects eventually present (as stereodefects and regiodefects). This has prevented the study of the effect of the sole comonomeric units on the crystallization behavior of iPB. As in the case of stereodefective samples of iPB prepared with metallocene catalysts, the use of metallocene catalysts has allowed to synthesize copolymers of iPB with macromolecules featured by a perfect statistical distribution of comonomeric units along the chains, a uniform comonomer concentration, and a negligible concentration of stereodefects.[94,95] This have allowed studying the influence of the single constitutional defect on the polymorphic behavior, on the rate of the phase transformation and mechanical properties of iPB.[94,95]

The examples of copolymers of iPB with ethylene[94] or long octene[95] comonomeric units are summarized. Samples of butene-ethylene (iPBEt) and butene-octene (iPBC8) copolymers were prepared with the catalyst **2** of Figure 8.[94,95] As described above, this catalyst is

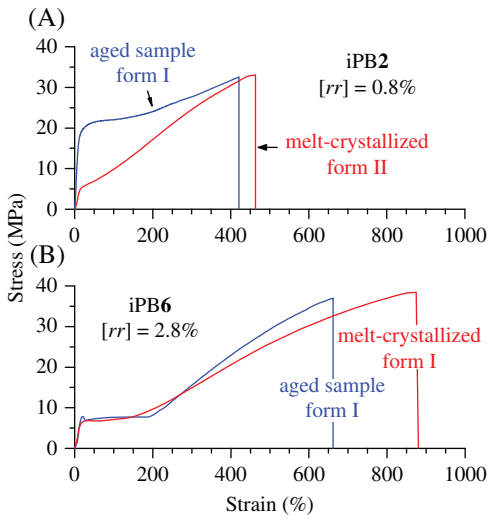

FIGURE 15 Stress strain curves of melt-crystallized samples (red lines) and of the same samples after aging at room temperature for 1 month (blue lines) of samples iPB**2** with [*rr*] = 0.8% (A) and iPB**6** with [*rr*] = 2.8% (B).[28]
Reproduced with permission from Ref. [28]. Copyright 2009 by Wiley VCH

isoselective and produces highly stereoregular iPB homopolymer and copolymers.[27] The negligible amount of stereodefects, the absence of regiodefects, the high molecular mass, the random distribution of ethylene units in iPBEt copolymers and octene units in iPBC8 copolymers and the broad range of concentration of the comonomeric units have allowed highlighting the effects of the sole ethylene or octene constitutional defects on the crystallization behavior and mechanical properties of iPB.[94,95]

2.2.1 | Butene-ethylene copolymers

The diffraction profiles of samples of iPBEt copolymers melt-crystallized and aged at 25°C are shown in Figure 16A,B, respectively.[94] The diffraction profiles of the homopolymer sample, corresponding to the highly isotactic sample iPB**2** of Figure 9, prepared with the catalysts **2** of Figure 8, are also reported for comparison (profiles a of Figure 16A,B). It is apparent that, while the homopolymer crystallizes from the melt in form II (profile a of Figure 16A), the iPBEt copolymers with low ethylene concentrations crystallize from the melt as mixtures of forms I and II (profiles b-e of Figure 16A),[94] and the sample with ethylene content of 5.7 mol% crystallizes directly in form I′ (profile f of Figure 16A). Samples with higher ethylene concentrations do not crystallize from the melt (profiles g-m of Figure 16A).[94] Crystals of form II obtained from the melt completely transform into form I by aging (profiles a-e of Figure 16B) at 25°C in aging time that becomes shorter with the increase of ethylene content. Finally, the amorphous samples, with high ethylene concentrations crystallize upon aging in form I′ (profiles g-l of Figure 16B). The amount of crystals of form I′, with respect to those of form II, in samples crystallized from the melt and from the amorphous of Figure 16, evaluated from the intensities of the $(110)_I$ and $(200)_{II}$ reflections of form I and form II at 2θ = 9.9° and 11.9°, respectively, increases with the increase of ethylene units (Figure 17A).[94] The rate of transformation of form II into form I at 25°C, evaluated from the amount of crystals of form I that develop during aging (Figure 17B), increases with the increase of ethylene concentration (Figure 17C), and is always faster than that observed in samples of copolymers prepared with Ziegler-Natta catalysts, reported in Ref.[92] (Figure 17C).

These data demonstrate that, as in the case of *rr* stereodefects, the ethylene comonomeric units induces crystallization of form I′ from the melt and from the amorphous state and increase the rate of transformation of form II into form I.[94]

The effect of ethylene comonomeric units is, therefore, similar to that of the *rr* stereodefects and has been explained as due to increased flexibility of the chains and crystallization kinetics of form I, and the reduced stability of form II.[94] As also shown in Figure 17C, this behavior is different from that observed in butene-ethylene copolymers synthesized with Ziegler-Natta catalysts[92,93] that still crystallize in form II even at high ethylene concentrations (up to 2.2 mol%) and only for ethylene content of ≈10 mol% a small amount of form I appears in the samples crystallized form the melt.[92,93] This is due to the nonrandom distribution of the ethylene comonomeric units in the Ziegler-Natta samples that makes the regular sequences of butene units still long, even for high defects concentration, able to crystallize in form II.[94]

2.3 | Butene-octene copolymers

Butene-ethylene copolymers (iPBC8) synthesized with the same catalyst **2** of Figure 8 have shown a crystallization behavior different from

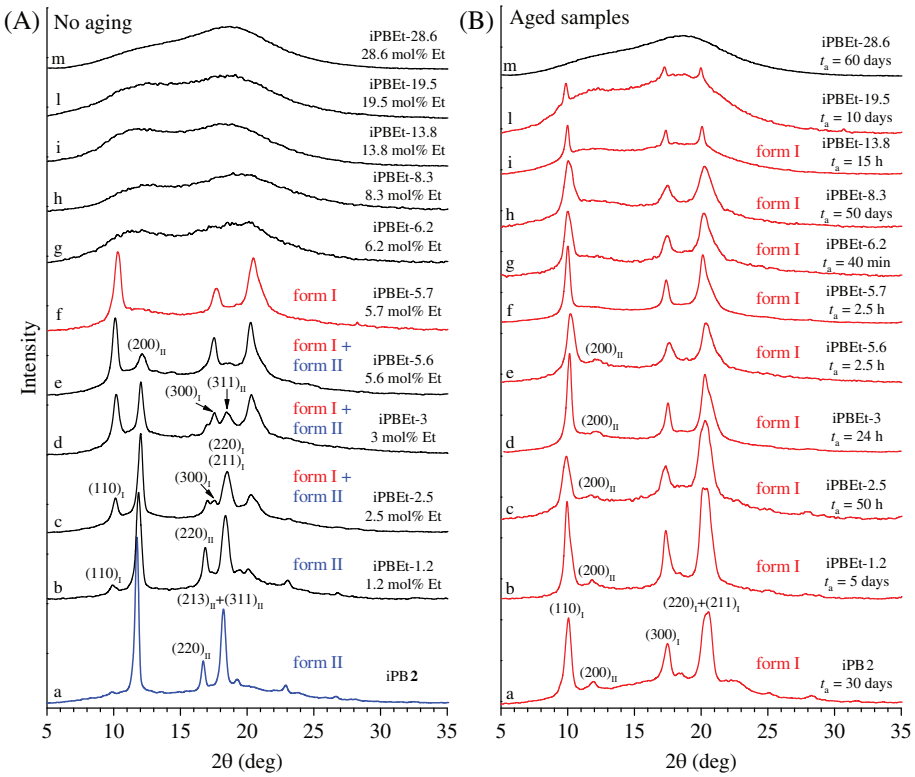

FIGURE 16 X-ray diffraction profiles of samples of iPBEt copolymers melt-crystallized (A) and aged at 25°C for the aging times t_a (B).[94] Reproduced with permission from Ref. [94]. Copyright 2014 by American Chemical Society

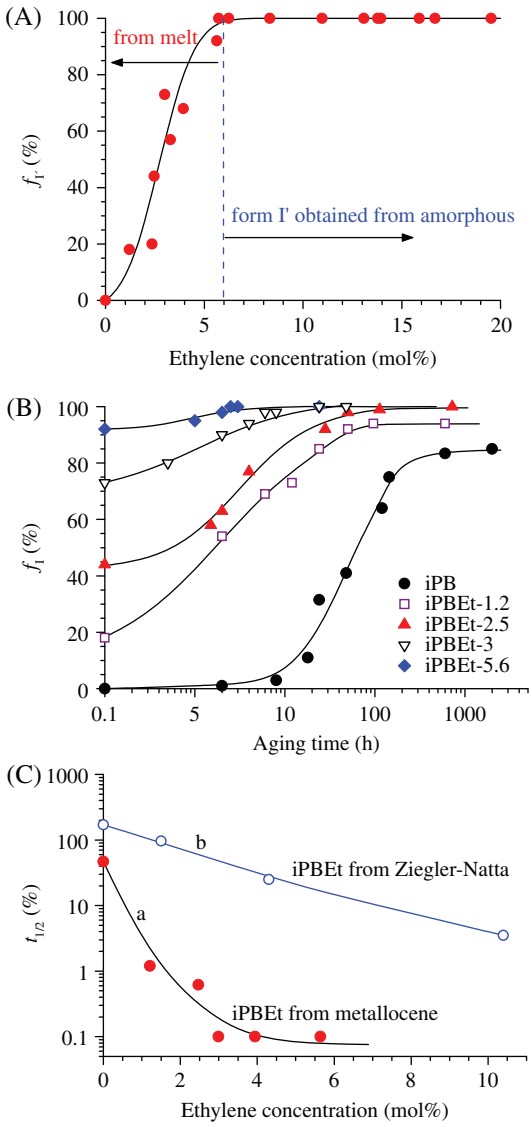

FIGURE 17 (A) Fractional amount of form I′ (f_I) initially crystallized from the melt in iPBEt copolymers (profile a-f of Figure 16A), and crystallized during aging from the amorphous (profiles g-l of Figure 16B)[94]. (B) Values of fraction of crystals of form I obtained from transformation of form II upon aging (profile a-f of Figure 16A,B) as a function of aging time, and (C) corresponding half transformation time ($t_{1/2}$)[94], compared with that of Ziegler-Natta iPBEt samples taken from ref. [92].
Reproduced with permission from Ref. [94]. Copyright 2014 by American Chemical Society

that of iPBEt samples.[95] The diffraction profiles of iPBC8 copolymers melt-crystallized and aged at 25°C for long time are shown in Figure 18A,B, respectively.[95] This time, all samples up to about 6 mol % of octene crystallize form the melt in form II, as the normal behavior of the iPB homopolymer (profiles a-g of Figure 18A).[95] The crystallinity decreases with the increase of concentration of octene units and the samples with octene concentration higher than 7 mol% no longer crystallize from the melt (profiles h-j of Figure 18A).

Figure 18B clearly shows that the transformation of form II into form I at 25°C occurs very slowly only for samples with low octene concentrations up to about 2.8 mol% (profiles b-d of Figure 18B). The aging time necessary to achieve complete transformation is very long (of the order of months), increases with the octene content, and is much longer than that necessary for iPBEt copolymers (Figure 16B).[95] For octene concentrations higher than 2-3 mol%, form II obtained from the melt (e-g of Figure 18A) is stable and does not transform into form I even for long aging time at room temperature (profile e-g of Figure 18B).[95] Samples that do not crystallize from the melt (for octene concentration higher than 7 mol%) (profile h-j of Figure 18A) crystallize by aging at 25°C as mixtures of crystals of forms II and I′ (profile h-i of Figure 18B).[95] The crystallized form II is stable and do not transform into form I by further aging for very long time.[95] Figure 19 shows that the fractional amount of form I in the samples aged for 3 years decreases with the increase of octene content up to about 7 mol% of octene[95] and then increases for higher octene content when form I′ crystallize from the amorphous phase. In the range 4-7 mol% of octene concentration, form II crystallized form the melt is stable and no form I is observed in the aged samples.[95]

The stabilization of form II in a defined range of octene concentration is confirmed by data of X-ray fiber diffraction patterns of samples of iPBC8 copolymers stretched at high degrees of deformation of Figure 20. It is known that form II crystallized form the melt in iPB homopolymer rapidly transforms into form I also by stretching.[30] The data of Figure 20 shows that only for the sample with low octene concentration form II transforms into form I by stretching (Figure 20A,B), as in the iPB homopolymer.[95] For higher octene concentrations, form II is stable even upon stretching and at high degree of deformation does not transform into form I but oriented fibers of form II are obtained (Figure 20C,D).[95]

The data of Figure 18–20 indicates that, contrary to ethylene units, octene units for concentrations higher than a threshold stabilizes the form II of iPB. This has been explained as due to the effect of stabilization of the 11/3 helical conformation that becomes more stable than the 3/1 helix of form I in the presence of bulky octene units randomly distributed along the iPB chains.[1,95]

The two reported examples of copolymers of iPB with ethylene and octene and the case of stereodefective homopolymer demonstrate how the crystallization behavior and polymorphism of a polymer may be altered in different ways for the presence of different types of defects. The presence of defects and of disorder may drive the crystallization toward one polymorphic form for both thermodynamic and kinetic effects resulting in the modification of the crystallization pathway delineated by the schemes of Figure 1.

3 | SYNDIOTACTIC POLYSTYRENE

Syndiotactic polystyrene (sPS) presents a complex polymorphism complicated by the presence of structural disorder.[96–117] It is another example of conformational polymorphism. Five different crystalline forms defined, α form,[97,98,110] β form,[102,104] γ form,[96] δ form,[109] and ε form,[111] two mesomorphic forms,[112–114] and various clathrates forms,[105–107] have been described. The most stable αand β forms crystallize with chains in *trans*-planar conformation.[96–98,102,104,110] The crystalline γ form and the nanoporous δ and ε forms are characterized by chains in **s**(2/1)2 helical conformation.[96,109,111] Moreover, sPS forms host-guest compounds (clathrate structures) with several organic

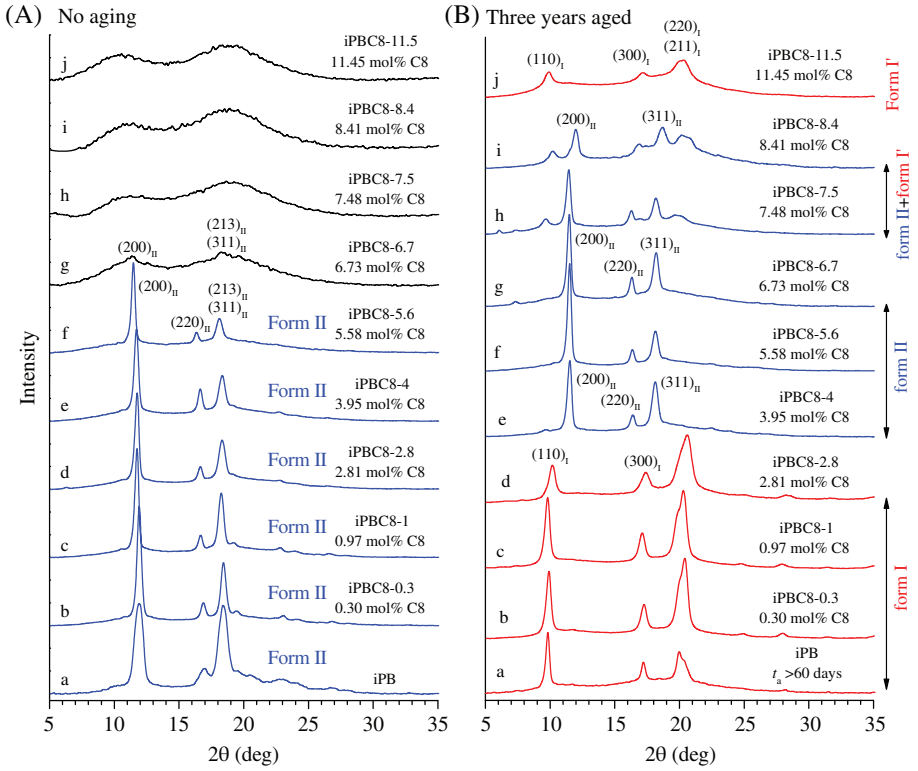

FIGURE 18 X-ray diffraction profiles of samples of iPBC8 copolymers melt-crystallized (A) and aged at 25°C for long time (B).[95] Reproduced with permission from Ref. [95]. Copyright 20 154 by Elsevier

and inorganic low molecular mass substances, all characterized by chains in s(2/1)2 helical conformation.[105–107,111]

The conformational polymorphism and the relative stabilities of the different polymorphic forms are in agreement with calculations of conformational energy.[115] The map of the conformational energy shows, indeed, an absolute minimum for a trans-planar conformation ($\theta_1 \approx \theta_2 \approx = 180°$) of the stable α and β forms, and a second relative minimum for the 2-fold helical conformation ($\theta_1 \approx 60°$ and $\theta_2 \approx 180°$ or $\theta_1 \approx 180°$ and $\theta_2 \approx -60°$) of the metastable γ and δ forms.[115] Models of the *trans*-planar and s(2/1)2 helical conformations of sPS are shown in Figure 21.

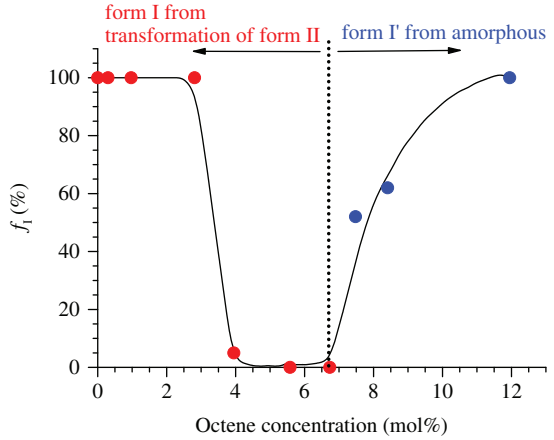

FIGURE 19 Values of the fractional amount of form I (●) and form I′ (●) (f_I) in the aged samples of Figure 18B as a function of octene concentration.[95] Reproduced with permission from Ref. [95]. Copyright 20154 by Elsevier)

Models of packing of the chains in the crystal structures of α form, β form and δ form of sPS are shown in Figure 22.[101,102,109] In the α form (Figure 22A), chains in *trans*-planar conformation are packed in a trigonal unit cell with axes a = 26.26 Å, b = 26.26 Å, and c = 5.04 Å with the space group symmetry $P3$.[100,101,110] In the β form, the same trans-planar chains are packed in an orthorhombic unit cell with axes a = 8.81 Å, b = 28.82 Å, and c = 5.1 Å with a space group $P2_12_12_1$ (Figure 22B).[102,104] In the nanoporous δ form, the chains in s(2/1)2 helical conformation are packed in a monoclinic unit cell with axes a = 17.4 Å, b = 11.85 Å, c = 7.70 Å, γ = 117° and space group $P2_1/a$ (Figure 22C).[109] The structure of δ form is characterized by the presence of empty cavities (the crystal density is ≈0.98 g/cm^3, smaller than that of the amorphous phase ≈1.05 g/cm^3), that can host low-molar-mass guest molecules forming clathrates structures.[109]

The stable α and β forms generally crystallize from the melt and present high melting temperatures (≈270°C), whereas the δ form and clathrate structures can be obtained by crystallization form various solvents.[96,105–107,109] γ and δ forms and clathrates structures are metastable and transform into the stable α form by heating.[96] δ form and clathrate samples transform into γ form at temperatures of nearly 130°C, and the γ form transforms into α form at higher temperatures of 180°C.[96,109,112] The polymorphism of sPS is, therefore, a case of enantiotropic polymorphism of the type of Figure 1B. The nanoporous δ form or the clathrates forms (in the presence of solvent or guest molecules that occupy cavities of the nanoporous structure) are stable at room temperature.[96] At higher temperatures, the γ form is stable in the range 130°C-180°C, and the α form is stable at temperature higher than 180°C before its melting at 270°C.[96]

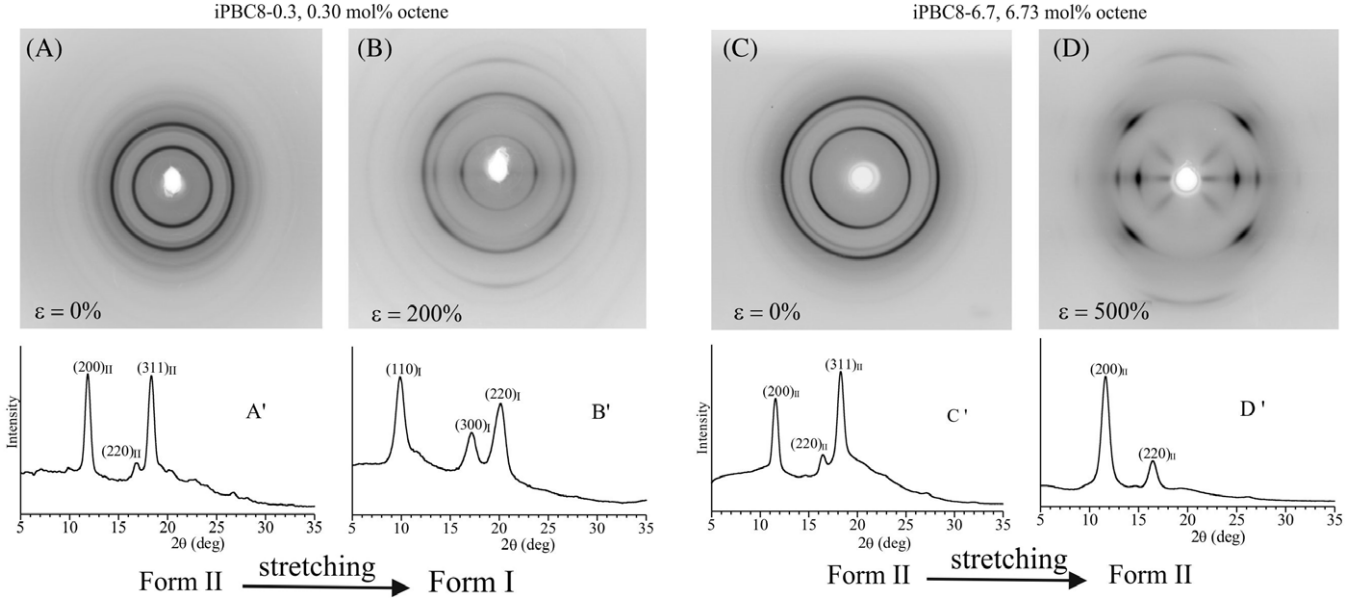

FIGURE 20 X-ray diffraction patterns of fibers of the samples of iPBC8 copolymers with 0.3 mol% (A,B) and 6.73 mol% (C,D) of octene stretched at the indicated values of deformations ε[95]
Reproduced with permission from Ref. [95]. Copyright 20154 by Elsevier)

The polymorphism of sPS is an interesting case of crystallization pathway that depends on various thermodynamic and kinetic factors and, in the crystallization from the melt, on the thermal history of the melt and the memory of crystals that persists in the melt even at high temperatures.[96] Moreover, this is a further example of polymorphism that arises because of the development of structural disorder and

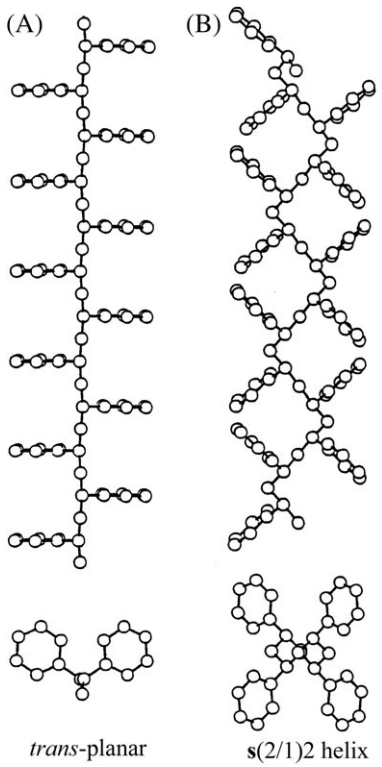

FIGURE 21 Models of the *trans*-planar conformation (A) and **s**(2/1)2 helical conformation (B) of sPS.
Reproduced with permission from Ref. [1]. Copyright 2014 by Wiley & Sons

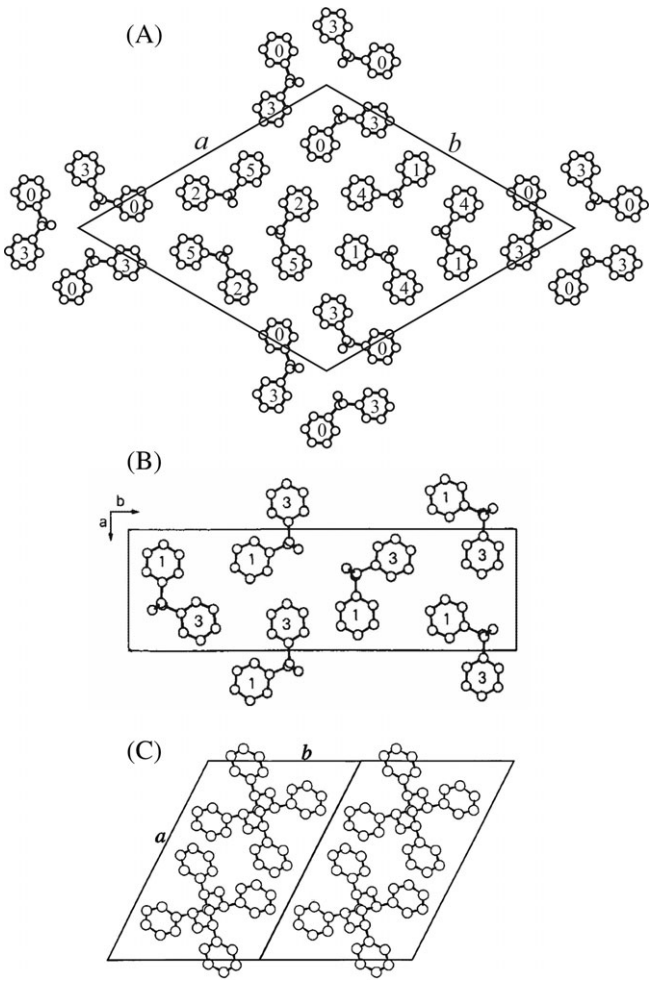

FIGURE 22 Models of packing of α form (A), β form (B), and δ form (C) of sPS[101,102,109]. The numbers inside the phenyl rings indicates the relative heights of the centers of phenyl rings in units *c*/6 in A for the α form and units *c*/4 in B for the β form, with *c* the chain axis.

crystallization of disordered structures. [1] The cases of α and β forms are illustrated in more details.

The crystallization of α and β forms from the melt strongly depends on the experimental conditions,[96] in particular, on the temperature of the melt, the time of permanence of the melt at that temperature, the crystallization temperature in the case of isothermal crystallizations, the cooling rate and the initial polymorphic form that is melted.[96,97] A pure β form crystallizes from the melt only when the temperature of the melt is very high and the melt is kept at this temperature for long time, that is, when in the melt there is no memory of the crystals of α form.[96] The α form crystallizes from the melt, instead, when the melt contains a memory of crystals of the α form, that is, when the temperature of the melt is low.[96] Moreover, α form crystals are obtained by fast cooling from the melt [96,102], and by cold crystallization from the quenched amorphous glass.[96,116]

Studies of the crystallization of α and β forms and of the influence of the parameters of the melt-crystallization have been reported by Woo et al. [97,118–123] The β form is favored for high crystallization temperatures (>260°C), whereas α form is favored at lower crystallization temperatures (<230°C)[97,118–125] and cold-crystallization from the amorphous phase.[96,97]

However, it has been reported that in the range of crystallization temperatures 230°C-260°C, the crystallization of α and β forms is mainly dependent on the maximum temperature of the melt (T_{max}).[126] For high T_{max} values, at least 50°C above the melting point of the starting polymorphic form, the β form always crystallizes for any crystallization temperature and polymorphic form of the starting sample.[126] For lower T_{max} values, the polymorphic form that crystallizes does not depend on the crystallization temperature but depends on the polymorphic form of the starting sample.[126] If the starting sample is initially in the β form, crystallization of the β form always occurs, whereas if the starting sample is in the α form, for low values of T_{max} crystallization of α form occurs.[126] At high values of T_{max}, higher than 280°C, the α and β forms crystallize in mixture. Therefore, the pure α form crystallizes only in the presence of a memory of crystals of α form in the melt, whereas β form always crystallizes when this memory is erased.[126]

The effect of structural disorder on the crystallization of α and β forms has been rationalized resorting to the concept of limit ordered and limit disordered model structures.[1] The crystal structures of α and β forms of Figure 22A,B have been described as a continuum of disordered modifications intermediate between limit disordered models (α' and β' ideal structures) and limit ordered models (α" and β" ideal structures).[96,100–102] In fact, depending on the condition of crystallization ordered or disordered modifications of α and β forms have been obtained.[96] In particular, by crystallization from the melt modifications of the α and β forms similar to the limit ordered α" structure and limit disordered β' structure, respectively, are obtained.[96] Modifications of the α form similar and closer to the limit disordered α' ideal structure are obtained by annealing of the amorphous phase or of the γ form,[96,100,101] whereas modifications of the β form similar and closer to the limit ordered β" ideal structure crystallize from solutions.[102] These complex behaviors have been explained by describing the disorder in the crystals of α and β forms and considering the disorder as a structural feature.[1]

In the case of the α form, the most important feature of the ordered model of the crystal structure (α" model) (Figure 22A) is that

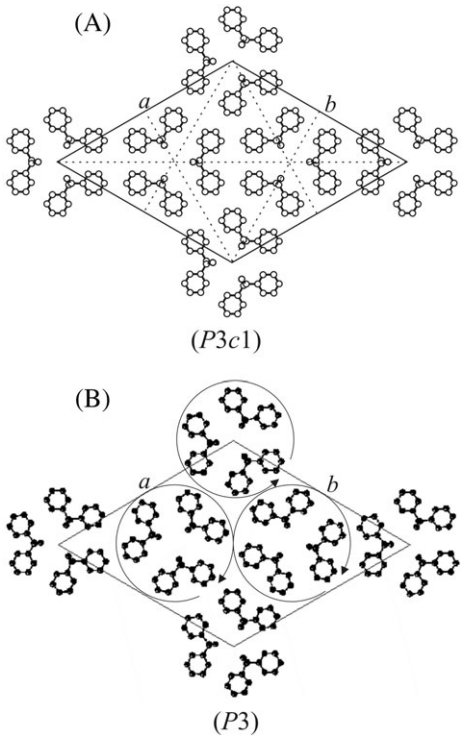

FIGURE 23 Models of the crystal structure of the α form of sPS with space group symmetries *P*3*c*1[100] (A) and *P*3[101,110] (B). Reproduced with permission from Ref. [1]. Copyright 2014 by Wiley & Sons

the *trans*-planar chains are organized in triplets around a 3-fold axis.[99] A model of packing that accounts for the experimental diffraction data [99–101,110] is characterized by a packing of triplets of *trans*-planar chains in a trigonal unit cell with space groups *P*3*c*1 or *P*3 (Figure 23).[100,101] In the model corresponding to the space group *P*3*c*1, the glide plane of the chains is also a crystallographic symmetry of the lattice[100] (Figure 23A). From detailed analysis of the electron diffraction patterns of single crystals[99,110] a model of low symmetry *P*3 has been proposed (Figure 23B).[101,110] In the space group *P*3, the crystallographic glide planes of the space group *P*3*c*1 are absent, therefore, the local glide plane of the chains is no longer a crystallographic symmetry[101] and the three triplets of chains may rotate around the 3-fold axes[101] and, assume different and independent orientations (Figure 23B).[110] This structure is, therefore, an example of symmetry breaking, where the local symmetry of the chains is lost in the lattice.[1] Samples of sPS crystallize from the melt in ordered modifications close to this limit ordered α" model of Figure 23.

Depending on the condition of crystallization the structure of Figure 23 presents structural disorder. In fact the α form that crystallizes by annealing the amorphous phase shows a diffraction profile different from that of the α form crystallized from the melt,[96,100] with systematic absence of *hkl* reflections with $-h + k + l \neq 3n$.[96,100,101] This has been explained assuming that the α form that crystallizes from the amorphous contains disorder that produces a statistical rhombohedral symmetry of the lattice.[100,101] A model of structural disorder of Figure 24 has been proposed.[100,101,127] *Trans*-planar sPS chains are clustered in triplets around 3-fold axes located in the

positions of the unit cell (0,0,*z*), (1/3,2/3,*z*), (2/3,1/3,*z*) (Figures 23A,B and 24A). As shown in Figure 25A,B, the triplets of chains assume in the unit cell two different orientations,[96,100] in which the benzene rings are in the same position, whereas the backbone atoms are rotated by 60°.[96,100,101,127] In the limit ordered α" modification of Figures 23 and 24A the three triplets of chains have three independent rotations[100,101,110] and the lattice has a trigonal, quasi-rhombohedral symmetry *P*3 (Figure 24A).[101,110] In the limit disordered α' modification, a statistical disorder between the two isosteric orientations of triplets of chains is present (Figure 24B).[100,127] The benzene rings are in positions similar to that in the limit ordered model and the backbone atoms assume statistically the six positions around the 3-fold axes, as in Figure 25C). Therefore, the limit disordered α' modification has a statistical full rhombohedral symmetry and can be described by the statistical space group $R\bar{3}$.[96,100,101,127] According to the model of disorder of Figure 24, crystals of the α form of sPS may be described with crystal modifications intermediate between the ideal ordered model (Figure 24A) and disordered model (Figure 24B). Crystallization from the melt gives ordered modifications of the α form similar to the limit ordered α" model of Figure 24A (space group *P*3), whereas annealing of the amorphous phase produces disordered modifications similar to the limit disordered model of Figure 24B (space group $R\bar{3}$).[96,100,101,127]

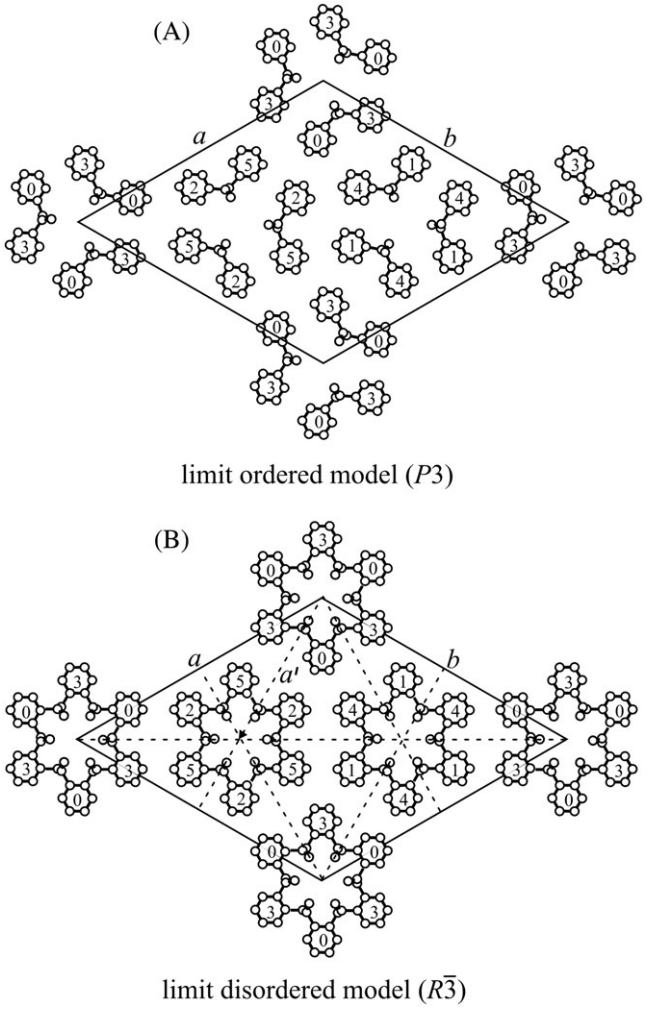

FIGURE 24 Models of the crystal structure of the α form of sPS described by the ideal limit ordered model (α"form, space group *P*3) (A) and the ideal limit disordered model (α' form, space group $R\bar{3}$) (B)[100,101,110,127]. The numbers inside the phenyl rings indicates the relative heights of the centers of phenyl rings in units *c*/6 with *c* the chain axis

Reproduced with permission from Ref. [1]. Copyright 2014 by Wiley & Sons

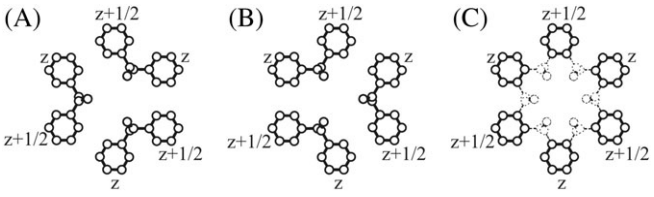

FIGURE 25 Different orientations of triplets of chains of sPS (A and B) assumed in the structure of the α form (Figures 22A, 23–24)[96,100,101,127] and statistical disordered orientation (C).

Reprinted with permission from Ref. [101]. Copyright 1996 by the American Chemical Society

It is worth noting that in this complex structure of the α form of sPS (Figures 23 and 24), the disorder in the positioning of the atoms of the backbone and a regular packing of a structural motif (the benzene rings), produce a mode of packing of the benzene rings very similar to that present in the crystal structure of isotactic polystyrene (iPS) (Figure 26), where chains in 3/1 helical conformation are packed in a trigonal unit cell with space groups *R*3*c* or $R\bar{3}c$ (Figure 26A).[128]

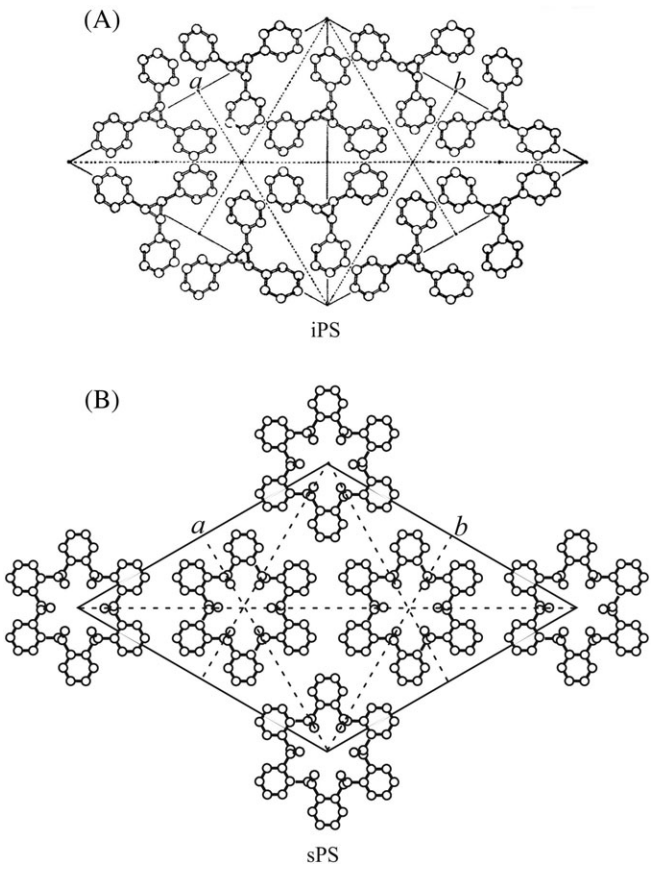

FIGURE 26 Models of the crystal structures of iPS (A) (space groups *R*3*c* or $R\bar{3}c$)[128] and α form of sPS (B) (space group $R\bar{3}$)[100,101,127]. The structures are characterized by a similar mode of packing of benzene rings

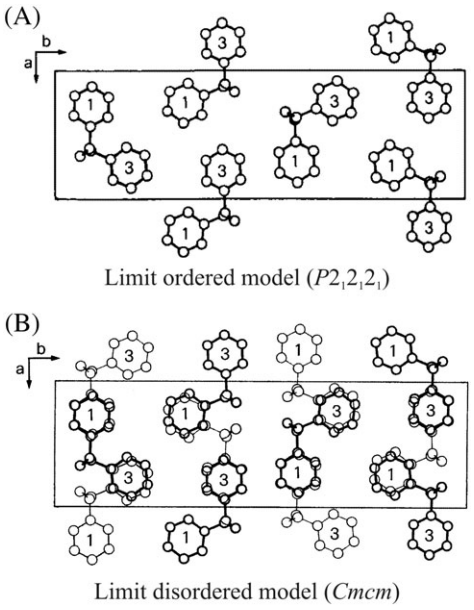

FIGURE 27 Limit ordered model (β" form, space group $P2_12_12_1$) (A) and limit disordered model (β' form, space group *Cmcm*) (B) for the crystal structure of the β form of sPS[102]. The numbers inside the phenyl rings indicate the relative heights of the centers of phenyl rings in units *c*/4 with *c* the chain axis. Reprinted with permission from Ref. [102]. Copyright 1992 by Elsevier Science

In the case of β form of sPS a different type of disorder is present which determines development of polymorphism with the presence of different modifications characterized by different degree of order.[102] This has been demonstrated by the fact that the β form crystallized form the melt shows diffraction profiles with systematic absence of the *hk*0 reflections with $h + k = 2n + 1$ [102,128]. A model of the structural disorder is shown in Figures 27 and 28. The limit ordered structure of Figure 27A (β" form, space group $P2_12_12_1$) corresponds to a regular succession of *ac* bilayers ABABAB in the model of Figure 28A. Disorder arises because defects in the regular alternation of *ac* bilayers of chains A and B along the *b* axis may be present as in the model of Figure 28B.[102] The statistical stacking of *ac* layers of chains along *b* produces a fully disordered structure of Figure 27B (β' form) that can be described by the ideal statistical space group *Cmcm*.[102] Modifications corresponding to the disordered model of Figure 28B are intermediate between the ideal ordered and disordered models of Figure 27. Crystallization of sPS from the melt gives modifications of β form similar to the limit disordered model (β' form) of Figure 27B, whereas samples crystallized by casting from solutions are in modifications similar to the limit ordered model (β" form) of Figure 27A.

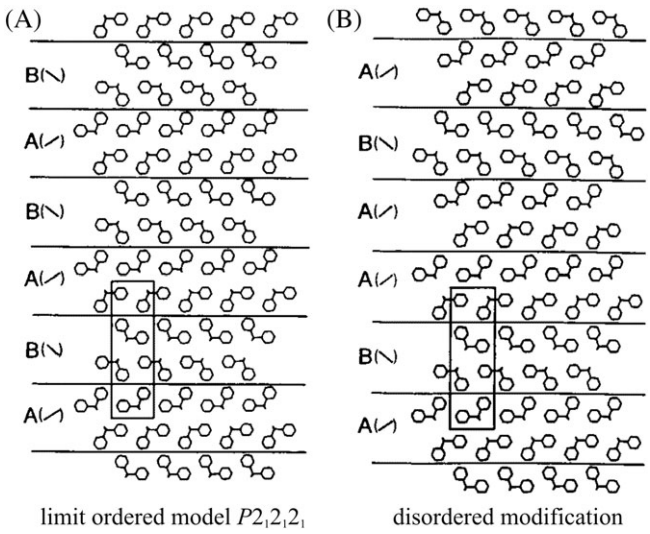

FIGURE 28 Model of structural disorder that develops in the β form of sPS.[102]. (A) Limit ordered model (β"form, space group $P2_12_12_1$) and (B) disordered modification containing defects in the stacking of *ac* layers along *b*.
Reprinted with permission from Ref. [102]. Copyright 1992 by Elsevier Science

4 | CONCLUSIONS

We analyze the thermodynamic basis for conformational and packing polymorphisms of polymers and several parameters and phenomena that influence the mode of packing of macromolecules and their role on driving crystallization of a particular polymorph are described. In particular, we show that the presence of defects and disorder in the crystals may alter the crystallization pathway through modification of the thermodynamic stability of the polymorphic forms and/or the kinetics of crystallization. Moreover we show that polymorphism often arises from crystallization of disordered structures. The cases of polymorphism and crystallization behavior of isotactic poly(butene) (iPB) and syndiotactic poly(styrene) (sPS) are analyzed in details as examples.

In the case of iPB, the effect of the presence of defects of stereoregularity and of constitutional defects, as comonomeric units, on the crystallization of forms I and II is described and taken as example of the alteration of the crystallization behavior because of the modification of both thermodynamic stability and kinetics of crystallization from the melt of the polymorphic forms. In particular, the presence of stereodefects and ethylene comonomeric units favors the crystallization from the melt of the stable form I, due to the increase of the crystallization kinetics of form I and the decrease of the thermodynamic stability of form II. The presence of octene comonomeric units instead increases the thermodynamic stability of form II that no longer transforms into form I at room temperature.

The case of sPS is taken as example of a very complex polymorphic behavior arising from the presence and development of structural disorder. The concepts of symmetry breaking in polymer crystals and that the presence of disorder in crystals is a rule rather than an exception, are illustrated. On these bases, a new view of the concepts of crystallinity and crystals in synthetic polymers is presented. The first concept is that crystallinity in polymeric materials is compatible with the absence of true 3-dimensional long-range order. Second, the disorder may be described as a structural feature. The crystal structures of semicrystalline polymers are discussed in terms of idealized limit ordered and limit disordered models of crystals, where long-range order may be achieved only for some structural features that are not necessarily coincident with single atoms.

ORCID

Claudio De Rosa http://orcid.org/0000-0002-5375-7475
Finizia Auriemma http://orcid.org/0000-0003-4604-2057

Anna Malafronte http://orcid.org/0000-0002-7854-5823
Miriam Scoti http://orcid.org/0000-0001-9225-1509

REFERENCES

[1] C. De Rosa, F. Auriemma. Crystals andCrystallinity in Polymers. *Diffraction Analysis of Ordered and Disordered Crystals*. John Wiley & Sons, Inc., Hoboken, **2014.**
[2] C. De Rosa, F. Auriemma. *Crystal structures of polymers*. In *Handbook of Polymer Crystallization*, Eds E. Piorkowska, G. C. Rutledge, John Wiley & Sons, Inc. Hoboken **2013**.
[3] P. Corradini, in *The Stereochemistry of Macromolecules*, Vol. 3, (Ed: A. D. Ketley), Marcel Dekker, Inc., New York **1968**, p. 1.
[4] P. Corradini, G. Guerra, *Adv. Polym. Sci.* **1992**, *100*, 182.
[5] C. De Rosa, *Topics in Stereochemistry* **2003**, *24*, 71.
[6] F. Auriemma, P. Corradini, C. De Rosa, *Adv. Polym. Sci.* **2005**, *181*, 1.
[7] L. Mandelkern, *Crystallization of Polymers. Equilibrium Concepts*, Vol. 1, University Press, Cambridge (UK) **2002**.
[8] H. Tadokoro, *Structure of Crystalline Polymers*, New York, John Wiley & Sons **1979**.
[9] C. De Rosa, F. Auriemma, in *Understanding of Polymer Crystallization*, *Lect. Notes Phys*, G. Reiter and G. R. Strobl, eds., Springer-Verlag, Berlin, **2007**, Vol. 714, Chapter 17, p. 345.
[10] W. Ostwald, *Z. Phys. Chem* **1897**, *22*, 289.
[11] A. Keller, M. Hikosaka, S. Rastogi, A. Toda, P. J. Barham, G. Goldbeck-Wood, *G J. Mater. Sci.* **1994**, *29*, 2579.
[12] A. Keller, S. Z. D. Cheng, *Polymer* **1998**, *39*, 4461.
[13] S. Z. D. Cheng, L. Zhu, C. Y. Li, P. S. Honigfort, A. Keller, *Thermochim Acta* **1999**, *332*, 105.
[14] S. Z. D. Cheng, *Phase Transitions in Polymers: The Role of Metastable States*, Elsevier, Amsterdam **2008**.
[15] J. Bernstein, R. J. Davey, J.-O. Henck, *Angew. Chem. Int. Ed.* **1999**, *38*, 3440.
[16] D. Cavallo, G. C. Alfonso, In *Polymer Crystallization II, from Chain Microstructure to Processing*, Eds. F. Auriemma, G. C. Alfornso, C. De Rosa. Springer-Verlag, Berlin. *Adv. Polym. Sci.* **2017**, *277*, 1.
[17] L. Yu, *CrstEngComm* **2007**, *9*, 847.
[18] P. Corradini, F. Auriemma, C. De Rosa, *Acc. Chem. Res.* **2006**, *39*, 314.
[19] K. Asai, *Polymer* **1982**, *23*, 391.
[20] C. De Rosa, F. Auriemma, C. Perretta, *Macromolecules* **2004**, *37*, 6843.
[21] C. De Rosa, F. Auriemma, A. Di Capua, L. Resconi, S. Guidotti, I. Camurati, I. E. Nifant'ev, I. P. Laishevtsev, *J. Am. Chem. Soc.* **2004**, *126*, 17040.
[22] C. De Rosa, F. Auriemma, G. De Lucia, L. Resconi, *Polymer* **2005**, *46*, 9461.
[23] C. De Rosa, F. Auriemma, *J. Am. Chem. Soc.* **2006**, *128*, 11024.
[24] C. De Rosa, F. Auriemma, *Prog. Polym. Sci.* **2006**, *31*, 145.
[25] C. De Rosa, F. Auriemma, O. Ruiz de Ballesteros, *Chem. Mat.* **2006**, *18*, 3523.
[26] C. De Rosa, F. Auriemma, O. Ruiz de Ballesteros, *Phys.Rev.Lett.* **2006**, *96*, 167801.
[27] L. Resconi, I. Camurati, F. Malizia, *Macromol. Chem. Phys.* **2006**, *207*, 2257.
[28] C. De Rosa, F. Auriemma, L. Resconi, *Ang. Chem. Int. Ed.* **2009**, *48*, 9875.
[29] C. De Rosa, F. Auriemma, O. Ruiz de Ballesteros, F. Esposito, D. Laguzza, R. Di Girolamo, L. Resconi, *Macromolecules* **2009**, *42*, 8286.
[30] C. De Rosa, F. Auriemma, M. Villani, O. Ruiz de Ballesteros, R. Di Girolamo, O. Tarallo, A. Malafronte, *Macromolecules* **2014**, *47*, 1053.
[31] G. Natta, P. Corradini, I. W. Bassi, *Nuovo Cimento*, Suppl. **1960**, *15*, 52.
[32] G. Natta, P. Corradini, I. W. Bassi, *Die Makromol. Chem* **1956**, *21*, 240.
[33] A. Turner-Jones, *J. Polym. Sci. B* **1963**, *1*, 455.
[34] a) A. Turner-Jones, *Polymer* **1966**, *7*, 23. b) A. Turner-Jones, *J. Polym. Sci. B* **1965**, *3*, 591.
[35] V. Petraccone, B. Pirozzi, A. Frasci, P. Corradini, *Eur. Polym. J.* **1976**, *12*, 323.
[36] P. Corradini, V. Petraccone, B. Pirozzi, *Eur. Polym. J.* **1976**, *12*, 831.
[37] P. Corradini, R. Napolitano, V. Petraccone, B. Pirozzi, *Eur. Polym. J.* **1984**, *20*, 931.
[38] G. Cojazzi, V. Malta, G. Celotti, R. Zannetti, *Makromol. Chem.* **1976**, *177*, 915.
[39] D. L. Dorset, M. P. McCourt, S. Kopp, J. C. Wittmann, B. Lotz, *Acta Crystallogr.* **1994**, *B50*, 201.
[40] B. Lotz, A. Thierry, *Macromolecules* **2003**, *36*, 286.
[41] L. Luciani, J. Seppälä, B. Löfgren, *Prog. Polym. Sci.* **1988**, *13*, 37.
[42] V. F. Holland, R. L. Miller, *J. Appl. Phys.* **1964**, *35*, 3241.
[43] K. W. Chau, P. H. Geil, *J. Macromol. Sci. Phys.* **1984**, *B23*, 115.
[44] M. Tosaka, T. Kamijo, M. Tsuji, S. Kohjiya, T. Ogawa, S. Isoda, T. Kobayashi, *Macromolecules* **2000**, *33*, 9666.
[45] P. Corradini, C. De Rosa, G. Zhi, R. Napolitano, B. Pirozzi, *Eur. Polym. J.* **1985**, *21*, 635.
[46] M. Farina, *Top. Stereochem.* **1987**, *17*, 1.
[47] K. Mislow, P. Bickart, *Israel J. Chem.* **1976**/1977, *15*, 1.
[48] M. M. Green, J.-W. Park, T. Sato, A. Teramoto, S. Lifson, R. L. B. Selinger, J. V. Selinger, *Angew. Chem. Int. Ed.* **1999**, *38*, 3138.
[49] H. Sakakihara, Y. Takahashi, H. Tadokoro, N. Oguni, H. Tani, *Macromolecules* **1973**, *6*, 205.
[50] H. Tadokoro, *Polymer* **1984**, *25*, 147.
[51] J. Jaxques, A. Collet, S. H. Wilen, *Enantiomers, Racemates and Resolutions*, John Wiley & Sons, New York (USA) **1981**.
[52] S. V. Meille, G. Allegra, *Macromolecules* **1995**, *28*, 7764.
[53] J. Boor Jr., J. C. Mitchell, *J. Polym. Sci.: Part A* **1963**, *1*, 59.
[54] J. Powers, J. D. Hoffman, J. J. Weeks, F. A. Quinn Jr., *J. Res. Natl. Bur. Stand.* **1965**, *69A*, 335.
[55] R. J. Schaffhauser, *J. Polym. Sci. B* **1967**, *5*, 839.
[56] R. M. Gohil, M. J. Miles, J. Petermann, *J. Macromol. Sci. Phys.* **1982**, *B21*, 189.
[57] Y. Fujiwara, *Polym. Bull.* **1985**, *13*, 253.
[58] K. W. Chau, Y. C. Yang, P. H. Geil, *J. Mater. Sci.* **1986**, *21*, 3002.
[59] T. C. Hsu, P. H. Geil, *Polym. Commun.* **1990**, *31*, 105.
[60] R. L. Miller, V. F. Holland, *J. Polym. Sci. B* **1964**, *2*, 519.
[61] S. Kopp, J. C. Wittmann, B. Lotz, *J. Mater. Sci.* **1994**, *29*, 6159.
[62] B. Lotz, C. Mathieu, A. Thierry, A. J. Lovinger, C. De Rosa, O. Ruiz de Ballesteros, F. Auriemma, *Macromolecules* **1998**, *31*, 9253.
[63] A. J. Foglia, *J. Appl. Polym. Sci., Appl. Polym. Symp* **1969**, *11*, 1.
[64] F. Danusso, G. Gianotti, *Makromol. Chem.* **1963**, *61*, 139.
[65] F. Danusso, G. Gianotti, *Makromol. Chem.* **1965**, *88*, 149.
[66] C. Nakafuku, T. Miyaki, *Polymer* **1983**, *24*, 141.
[67] I. D. Rubin, J. Polym, *Sci., Polym. Lett* **1964**, *2*, 747.
[68] J. Boor Jr., E. A. Youngman, *J. Polym. Sci. B* **1964**, *2*, 903.
[69] a) T. Miyoshi, A. Mamun, D. Reichert, *Macromolecules* **2010**, *43*, 3986. b) T. Miyoshi, A. Mamun, *Polymer J.* **2012**, *44*, 65.
[70] P. H. Geil, K. W. Chau, A. Agarwal, C. C. Hsu, in *Morphology of Polymers*, (Ed: B. Sedlacek), Walter de Gruyter, Berlin **1986**, p. 87.
[71] K. W. Chau, P. H. Geil, J. Macromol, *Sci., Phys.* **1984**, *B23*, 115.
[72] a) S. Kopp, J. C. Wittmann, B. Lotz, *Polymer* **1994**, *35*, 908. b) S. Kopp, J. C. Wittmann, B. Lotz, *Polymer* **1994**, *35*, 916. c) C. Mathieu, W. Stocker, A. Thierry, J. C. Wittmann, B. Lotz, *B. Polymer* **2001**, *42*, 7033.
[73] C. D. Armeniades, E. Baer, *J. Macromol. Sci. Phys.* **1967**, *B1*, 309.
[74] C. Nakafuku, T. Miyaki, *Polymer* **1983**, *24*, 141.
[75] a) M. Yamashita, A. Hoshino, M. Kato, *J Polym Sci B* **2007**, *45*, 684. b) M. Yamashita, *J. Cryst. Growth* **2007**, *310*, 1739. c) M. Yamashita, *J. Cryst. Growth* **2009**, *311*, 556. d) M. Yamashita, *J. Cryst. Growth* **2009**, *311*, 560.
[76] B. Zhang, D. Yang, S. Yan, *J. Polym. Sci. Polym. Phys.* **2002**, *40*, 2641.
[77] F. Azzurri, A. Flores, G. C. Alfonso, F. J. Balta Calleja, *Macromolecules* **2002**, *35*, 9069.
[78] F. Azzurri, A. Flores, G. C. Alfonso, I. Sics, B. S. Hsiao, F. J. Balta Calleja, *Polymer* **2003**, *44*, 1641.
[79] G. C. Alfonso, F. Azzurri, M. Castellano, *J. Therm. Anal.Calorim.* **2001**, *66*, 197.
[80] M. Kaszonyiova, F. Rybnikar, P. H. Geil, *J. Macromol. Sci. Phys.* **2004**, *B43*, 1095.
[81] K. Hong, J. E. Spruiell, *J. Appl. Polym. Sci.* **1985**, *30*, 3163.
[82] K. W. Chau, Y. C. Yang, P. H. Geil, *J. Mater. Sci.* **1986**, *21*, 3002.
[83] G. Gianotti, A. Capizzi, *Makromol. Chem.* **1969**, *124*, 152.
[84] K. Nakamura, T. Aoike, K. Usaka, T. Kanamoto, *Macromolecules* **1999**, *32*, 4975.
[85] J. M. Samon, J. M. Schultz, B. S. Hsiao, J. Wu, S. Khot, J. Polym, *Sci., Part B: Polym. Phys.* **2000**, *38*, 1872.
[86] K. Tashiro, J. Hu, H. Wang, M. Hanesaka, A. Saiani, *Macromolecules* **2016**, *49*, 1392.

[87] F. M. Su, X. Y. Li, W. M. Zhou, W. Chen, H. L. Li, Y. H. Cong, Z. H. Hong, Z. M. Qi, L. B. Li, *Polymer* **2013**, *54*, 3408.
[88] Y. Qiao, Q. Wang, Y. Men, *Macromolecules* **2016**, *49*, 5126.
[89] a) J. A. Ewen, *J. Am. Chem. Soc.* **1984**, *106*, 6355. b) H. H. Brintzinger, D. Fischer, R. Mulhaupt, B. Rieger, R. M. Waymouth, *Angew. Chem., Int. Ed. Engl.* **1995**, *34*, 1143.
[90] J. D. Hoffman, G. T. Davis, J. I. Jr. *Lauritzen, in Treatise on Solid State Chemistry, Hannay*, N. B. Ed., pp. 497–614. Plenum: New York, **1997**. J. D. Hoffman, R. L. Miller, *Polymer* **1997**, *38*, 3151.
[91] B. Wunderlich, *Macromolecular Physics*, Vol. 3, Academic Press, New York **1980**.
[92] F. Azzurri, G. C. Alfonso, M. A. Gómez, M. C. Martì, G. Ellis, C. Marco, *Macromolecules* **2004**, *37*, 3755.
[93] F. Azzurri, M. A. Gómez, G. C. Alfonso, G. Ellis, C. Marco, *J. Macromol. Sci. Phys.* **2004**, *B43*, 177.
[94] C. De Rosa, O. Ruiz de Ballesteros, F. Auriemma, R. Di Girolamo, C. Scarica, G. Giusto, S. Esposito, S. Guidotti, I. Camurati, *Macromolecules* **2014**, *47*, 4317.
[95] C. De Rosa, O. Tarallo, F. Auriemma, O. Ruiz de Ballesteros, R. Di Girolamo, A. Malafronte, *Polymer* **2015**, *73*, 156.
[96] G. Guerra, V. M. Vitagliano, C. De Rosa, V. Petraccone, P. Corradini, *Macromolecules* **1990**, *23*, 1539.
[97] E. M. Woo, Y. S. Sun, C. P. Yang, *Prog. Polym. Sci.* **2001**, *26*, 945.
[98] A. Immirzi, F. de Candia, P. Iannelli, A. Zambelli, V. Vittoria, *Makromol.Chem., Rapid Commun* **1988**, *9*, 761.
[99] O. Greis, Y. Xu, T. Asano, J. Petermann, *Polymer* **1989**, *30*, 590.
[100] C. De Rosa, G. Guerra, V. Petraccone, P. Corradini, *Polym.J.* **1991**, *23*, 1435.
[101] C. De Rosa, *Macromolecules* **1996**, *29*, 8460.
[102] C. De Rosa, M. Rapacciuolo, G. Guerra, V. Petraccone, P. Corradini, *Polymer* **1992**, *33*, 1423.
[103] Y. Chatani, Y. Shimane, Y. Inoue, T. Inagaki, T. Ishioka, T. Ijitsu, T. Yukinari, *Polymer* **1992**, *33*, 488.
[104] Y. Chatani, Y. Shimane, T. Ijitsu, T. Yukinari, *Polymer* **1993**, *34*, 1625.
[105] Y. Chatani, Y. Shimane, T. Inagaki, T. Ijitsu, T. Yukinari, H. Shikuma, *Polymer* **1993**, *34*, 1620.
[106] Y. Chatani, T. Inagaki, Y. Shimane, H. Shikuma, *Polymer* **1993**, *34*, 4841.
[107] C. De Rosa, P. Rizzo, O. Ruiz de Ballesteros, V. Petraccone, G. Guerra, *Polymer* **1999**, *40*, 2103.
[108] O. Tarallo, F. Auriemma, O. Ruiz de Ballesteros, R. Di Girolamo, C. Diletto, A. Malafronte, C. De Rosa, *Macromol. Chem. Phys.* **2013**, *214*, 1901.
[109] C. De Rosa, G. Guerra, V. Petraccone, B. Pirozzi, *B. Macromolecules* **1997**, *30*, 4147.
[110] L. Cartier, T. Okihara, B. Lotz, *B. Macromolecules* **1998**, *31*, 3303.
[111] V. Petraccone, O. Ruiz de Ballesteros, O. Tarallo, P. Rizzo, G. Guerra, *Chem. Mater.* **2008**, *20*, 3663.
[112] C. Manfredi, C. De Rosa, G. Guerra, M. Rapacciuolo, F. Auriemma, P. Corradini, *Macromol. Chem. Phys* **1995**, *196*, 2795.
[113] V. Petraccone, F. Auriemma, F. Dal Poggetto, C. De Rosa, G. Guerra, P. Corradini, *Makromol. Chem.* **1993**, *194*, 1335.
[114] F. Auriemma, V. Petraccone, F. Dal Poggetto, C. De Rosa, G. Guerra, C. Manfredi, P. Corradini, *Macromolecules* **1993**, *26*, 3772.
[115] P. Corradini, R. Napolitano, B. Pirozzi, *Eur. Polym. J.* **1990**, *26*, 157. R. Napolitano, B. Pirozzi, *Macromol. Theory Simul.* **1999**, *8*, 15.
[116] G. Guerra, C. De Rosa, V. M. Vitagliano, V. Petraccone, P. Corradini, F. E. Karasz, *Polym Commun* **1991**, *32*, 30.
[117] G. Guerra, C. De Rosa, V. M: Vitagliano, V. Petraccone, P. Corradini, *J. Polym. Sci: Part B: Polym Phys* **1991**, *29*, 265.
[118] E. M. Woo, F. S. Wu, *Macromol Chem Phys* **1998**, *199*, 2041.
[119] E. M. Woo, Y. S. Sun, M. L. Lee, *Polym. Commun* **1999**, *40*, 4425.
[120] Y. S. Sun, E. M. Woo, *Macromolecules* **1999**, *32*, 7836.
[121] R. H. Lin, E. M. Woo, *Polymer* **2000**, *41*, 121.
[122] R. M. Ho, C. P. Lin, H. Y. Tsai, E. M. Woo, *Macromolecules* **2000**, *33*, 6517.
[123] Y. S. Sun, E. M. Woo, *Polymer* **2001**, *42*, 2241.
[124] W. Bu, Y. Li, J. He, J. Zeng, *Macromolecules* **1999**, *32*, 7224.
[125] Y. Li, J. He, W. Qiang, X. Hu, *Polymer* **2002**, *43*, 2489.
[126] C. De Rosa, O. Ruiz de Ballesteros, M. Di Gennaro, F. Auriemma, *Polymer* **2003**, *44*, 1861.
[127] P. Corradini, C. De Rosa, G. Guerra, R. Napolitano, V. Petraccone, B. Pirozzi, *Eur. Polym. J.* **1995**, *30*, 1173.
[128] a) G. Natta, P. Corradini, *Makromol. Chem.* **1955**, *16*, 77. b) G. Natta, P. Corradini, I. W. Bassi, *Nuovo Cimento, Suppl* **1960**, *15*, 68.

AUTHOR BIOGRAPHIES

Claudio De Rosa is Full Professor of Macromolecular Chemistry at the University of Naples Federico II (Italy). He received the Master degree in Chemistry in 1983 and the PhD in Chemistry in 1989 from the University of Naples. His research activity comprises the study of the crystal structure and physical properties of polymers. He is author of about 290 papers.

Finizia Auriemma is Full Professor of Macromolecular Chemistry at the University of Naples Federico II (Italy). She received the Doctor degree in Chemistry in 1984 and the PhD in Chemistry in 1989 from the University of Naples. Her research activity comprises the study of the crystal structure of polymers and of the disorder in polymer crystals. She is author of about 200 papers.

Anna Malafronte is Researcher in Industrial Chemistry at the University of Naples Federico II (Italy). She graduated in Chemical Sciences at the University of Naples in 2011 and she got the PhD in Chemical Sciences in 2015 from the same University. Her main research interests are the study of periodic nanostructures formed through self-assembly of block-copolymers and of the relationships between the molecular structure and the physical properties of crystalline polymers.

Miriam Scoti is Post Doc at the University of Naples Federico II (Italy). She received the Master Degree in Chemical Sciences in 2014 and the PhD in Chemical Sciences in 2018 from the University of Naples. Her research interest is the study of the structure and morphology of crystalline polymers synthesized with organometallic catalysts and of the relationships between the molecular architecture induced by the catalysts and the crystalline structure and physical properties of polymers.

How to cite this article: De Rosa C, Auriemma F, Malafronte A, Scoti M. Crystal structures and polymorphism of polymers: Influence of defects and disorder. *Polymer Crystallization*. 2018;e10015. https://doi.org/10.1002/pcr2.10015